



# **OCEANS ENERGY FOR THE SOUTH AFRICA COASTLINE**

**By**

**MICHEE NTONTO LUNKAMBA**

**Thesis submitted in part-fulfilment of the requirements for the  
degree**

**Master of Engineering in Energy (MGENRC)**

**In the Faculty of Engineering and the Built Environment**

**At the Cape Peninsula University of Technology**

**Supervisor: Prof MTE Kahn**

**Bellville**

**15 February 2023**

## DECLARATION

I, Michee Ntonto Lunkamba, hereby declare that the contents of this dissertation or thesis represent my own unaided work and that the dissertation or thesis has not previously been submitted for academic examination toward any qualification. In addition, I further declare that the dissertation or thesis has not been submitted for academic examination toward any qualification in the past. Also, the ideas I express there are mine alone and don't always reflect the ideas of the Cape Peninsula University of Technology.

Signed:



Date: 15 February 2023

## Abstract

As a renewable power resource, South Africa is currently investing in solar and wind power, with ocean energy already undergoing research and development. This study aimed is to investigate and development of a comprehensive techno-economic model for the assessment of ocean energy technologies, with various aspects, including criteria for the assessment and improvement of some shortcomings found in other techno-economic studies.

Between the information required by the model and the actual information available in the case studies a relevant value of between 83 to 86 percent was found and the feasibility information provided by the model was thus demonstrated.

This dissertation discusses various methods, including three principal techniques for the collection of energy from the oceans: wave power, tide power, and ocean thermal energy conversion. These findings were then used to compare costs to other renewables and non-renewables. The dissertation ends with the limitations of the model and recommendations for research into the future.

## Acknowledgements

I am grateful to the Almighty for his inexhaustible blessings on my life, especially my education at Cape Peninsula University of Technology. These blessings were and continue to be displayed in the following ways:

I want to say thank you to everyone who has contributed their time and thought to making this study possible. My supervisor, Prof Khan, deserves special gratitude. I appreciate the confidence you have in my work and the drive you have shown throughout this challenging course. Without a doubt, his encouragement helped me stay committed to my study project.

I would like to thank my parents, Mr. Delphin Kazadi Buluma and Mrs. Beatrice Ebono Ntonto, my brothers Dr Savio Munga Buluma , Sam Kabale Buluma , and my sisters Moma Safi Consolate , Gloire Lubaba Buluma, Marie Christiane Ngiele Ngoie for their support and encouragement.

My research was made easy by the CPUT postgraduate award and research money, which provided me with a university bursary

# Table of Contents

DECLARATION .....	ii
<b>Abstract</b> .....	iii
Acknowledgements.....	iv
<b>Table of Figures</b> .....	viii
Table of Tables .....	x
<b>List of Definitions</b> .....	xi
1. Chapter One: Introduction.....	1
1.1. Background .....	1
1.2. Aims and objectives. ....	3
1.2.1. Aims.....	3
1.2.2. Objectives.....	3
1.3. Problem Statement.....	3
1.4. Research Methodology .....	4
1.5. Research Significance.....	4
1.6. Structural of thesis .....	4
2. Chapter Two: Literature review .....	6
2.1. Introduction .....	6
2.2. Wave energy .....	7
2.2.1. Background .....	7
2.2.2. Effective wave energy conversion .....	8
2.2.3. Calculations .....	9
2.3. Ocean current energy .....	10
2.3.1. Background .....	10
2.3.2. Observation.....	12
2.4. Tidal energy.....	13
2.4.1. Background .....	13
2.4.2. Methods of tide generations .....	14
2.5. Ocean thermal energy conversion.....	15
2.5.1. Background .....	15
2.5.2. An OTE Plant's Location and Potential Impacts .....	16
2.6. Marine winds energy .....	19
2.6.1. Background .....	19
2.6.2. Estimation of wind resources.....	20
2.7. Economic valuation of ocean energy .....	21

2.7.1.	Background .....	21
2.7.2.	Methodology and Data sources .....	22
2.8.	Conclusion.....	23
3.	Chapter Three: Selection and Comparison of technologies .....	24
3.1.	Background .....	24
3.2.	Comparison of technologies .....	27
3.3.	Ocean energy generating poses environmental challenges. ....	30
3.4.	Aspects of economics.....	31
3.5.	Conclusion.....	32
4.	Chapter Four: Analysis of measured wave and current data .....	34
4.1.	Port Nolloth.....	35
4.2.	Slangkop.....	35
4.3.	Cape Point .....	36
4.4.	FA platform .....	36
4.5.	Durban .....	36
4.6.	Wave height analysis .....	37
4.7.	Wave period analysis .....	38
4.8.	Wave power analysis .....	40
4.9.	Conclusion.....	40
5.	Chapter Five: The spatial distribution of wave power off South Africa's most active coastal zone 42	
5.1.	The study relied on data from offshore waves.....	42
5.1.1.	Wave data from the National Centre for Environmental Prediction (NCEP) off the coast of the United States.....	43
5.1.2.	Distribution of wave heights .....	44
5.2.	The SWAN wave model's history .....	45
5.3.	Methodology of wave transfer .....	45
5.4.	Input requirements for SWAN .....	46
5.5.	Validation of the model on the southwest coast.....	46
5.6.	Conclusion.....	48
6.	Chapter Six: Design .....	49
6.1.	Background of the design .....	49
6.1.1.	Life of design, return period, and likelihood of exceeding expectations.....	49
6.1.2.	Hydrographic conditions.....	49
6.1.3.	Water depth.....	49
6.1.4.	Tidal levels.....	50

6.1.5.	Storm surge.....	50
6.1.6.	Sea level rise.....	50
6.2.	Offshore design wave conditions.....	51
6.2.1.	Significant wave height .....	51
6.2.2.	Peak wave period.....	52
6.2.3.	Peak enhancement factor .....	52
6.2.4.	Directional spreading.....	52
6.3.	Nearshore design wave conditions.....	52
6.4.	Design wave loading and dimensional requirements.....	53
6.4.1.	Type of wave forces .....	54
6.4.2.	Failure modes.....	55
6.4.3.	Foundation design.....	55
6.4.4.	Material.....	55
6.4.5.	Wall thickness and structural height .....	55
6.4.6.	Pulsating wave loads.....	56
7.	Chapter Seven: Results and Discussion.....	57
7.1.	Outcomes of the model research .....	57
7.1.1.	average wave power per year.....	58
7.1.2.	Annual average wave power.....	62
7.1.3.	Monthly average wave power .....	62
7.2.	Model hind cast and observed data comparison.....	64
7.2.1.	Monthly wave power distribution at Cape Point was compared with data from SWAN hind cast transmissions at the latter recording point.....	64
8.	Chapter Eight: Conclusion and Recommendations.....	67
8.1.	Conclusion.....	67
8.2.	Recommendations for further research and improvements.....	68
	Reference.....	70

## Table of Figures

Figure 1: Bathymetry around South Africa .....	2
Figure 2: The current meter deployments' approximate locations.....	11
Figure 3: Ten minute sample ADCP speed data.....	13
Figure 4: The ADCP observation average signal strength reflects the high water clarity .....	13
Figure 5: Average correlation (%) for the ADCP observation .....	13
Figure 6: An OTE facility near the coast of Wright Canyon is depicted schematically (courtesy of Sea Solar Power, Jacobus, PA, USA) .....	17
Figure 7: An OTE plant's relative position and influence.....	18
Figure 8: composite false colour satellite image of sea surface temperatures on the provided scale, collected on July 31, 2020 (with thanks to the Marine Remote Sensing Unit).....	24
Figure 9: The temperature structure (°C) and accompanying currents with speed's' are shown in an offshore region at Port Edward (adapted from Pearce, 2019). .....	25
Figure 10: The South African coastline's average wave energy (from van Niekerk, 2012) .....	28
Figure 11: Wave parameters that are fundamental (CEM, 2006) .....	29
Figure 12: Southern African seabed contours to a depth of 3000 m .....	35
Figure 13: Slangkop and Cape Point wave recording stations' locations .....	36
Figure 14: the likelihood that $H_{m0}$ will be exceeded at each wave recording station .....	37
Figure 15: $H_{m0}$ incidence frequency over all wave recording stations.....	38
Figure 16: $T_p$ occurrence frequency at all wave recording stations.....	39
Figure 17: The southwest coastline region, Slangkop, and Cape Point wave recording stations are all indicated by the offshore NCEP data's relative location. On the computational border of the model, red circles denote SWAN input values.....	44
Figure 18: (a) The likelihood that the wave height at NCEP 340S 17.50E will be exceeded as recorded at the wave recording station at Cape Point. (b) Wave period frequency observed at the Cape Point wave recording station from July 2012 to July 2020 at NCEP 34S 17.....	45
Figure 19: From July 2010 to July 2019, the wave power at Cape Point and the closest model grid point averaged monthly median values. ....	47
Figure 20: Probability of exceeding wave strength at Cape Point and the closest model grid point from July 2012 to July 2018, as predicted and observed.....	48
Figure 21: For the 11-year NCEP data, maximum wave height per direction .....	51
Figure 22: a contour map showing the research area's bathymetry.....	58
Figure 23: Summertime spatial distribution of the mean seasonal average wave power (kW/m) .....	60
Figure 24: Seasonal average wave power (kW/m) for fall, distributed spatially.....	60



Figure 25: Winter-specific spatial distribution of the mean seasonal average wave power (kW/m) ...	60
Figure 26: Early summer annual mean energy production (kW/m) spatial dispersion.....	60
Figure 27: Seasonal likelihood of exceeding wave power at the nearest model grid cell to the Cape Point recording station .....	61
Figure 28: statistical characteristics of the predicted mean monthly wave power .....	62
Figure 29: Wave power average monthly averages for the several wave measurement sites.....	63
Figure 30: Mean monthly 90% likelihood of wave power exceedance readings for the various stations .....	63
Figure 31: Wave power monthly standard variation for the different stations .....	64
Figure 32: Wave power is measured and predicted monthly. ....	65
Figure 33: Wave power statistics recorded at the Cape Point recording station and the likelihood of exceeding it (hind cast data transferred).....	66

## Table of Tables

Table 1:Wave height, period, and power are statistical parameters that are averaged over a year...	26
Table 2:Information about wave recording stations that is relevant .....	34
Table 3:Measured wave data is used to create wave heights. ....	38
Table 4:The strength of the wave as a function of $T_p$ , $T_e$ , and $T_m$ .....	40
Table 5:Tidal levels forecast for Cape Town .....	50
Table 6:circumstances for offshore and nearshore waves in 100 years.....	52
Table 7:the Shore SWEC at Granger Bay's design standards.....	53
Table 8:Extreme seasonal wave power occurrences have a 6% and 2% chance of exceeding the model grid point nearest to the Cape Point recording station, respectively. ....	61
Table 9:Average monthly wave power of observed and simulated data that differs by a certain percentage .....	65

## List of Definitions

AP Acceleration Profile

CFD Computational Fluid Dynamics

DC Direct Current

DF Design Factor

FRF Frequency Response Function

FS First Script

LD Logarithmic Decrement

MRTD Maximum Relative Tip Displacement

OTE Ocean Thermal Energy

OTEC Ocean Thermal Energy Conversion

PE Piezoelectric Element

PV Photovoltaic

SAES South Africa Energy Statistics Year

# 1. Chapter One: Introduction

## 1.1. Background

It is possible to rely on ocean energy as a long-term solution to the energy dilemma. South Africa's marine domain and coastline are both sizable. There is a lot of room for growth in the world's energy sector. Therefore, the development of ocean energy is of great strategic importance for the future of South Africa. As a rule, large-scale, long-term testing at sea is required to evaluate the performance of an ocean energy extraction device before it can be used commercially. Costs, efficiency, and dependability are only a few of the economic assessment indicators that must be verified before the technology can be widely used in the commercial sector. So, in order to bring a technology for developing ocean energy to market, full-scale sea tests are needed.

It must be understood at the beginning that ocean conditions differ greatly across the globe, and an energy extraction suitable in one region is not feasible in another. Consequently, it is important to have a clear understanding of the ocean environment in the region to assess a specific oceanic process and its power generation potential. Consequently, to assess a particular oceanic process and its potential for generating power, it is necessary to have a good understanding of the ocean environment in the area. It means that each oceanographic region must be considered separately for each different energy source. considered here, specifically the following: Currents, tides, waves, wind, thermal.

Note that potential sources such as osmosis and oceanic biofuels are not included. In the case of wind energy, only the situation over the ocean itself will be considered, since there are several wind farms operating and being constructed on the adjacent land. Moreover, some of the five energy sources listed above may be interrelated, e.g., tides and currents, but in each case the primary phenomenon will be considered, and thus tidal currents will fall under tides. The ocean is a very harsh and dangerous environment, and any structures erected must be able to withstand extreme conditions.

Waves, winds, and currents have incredible destructive power, but it is not only during storms that failure can occur day to day maintenance is essential to counter the continuous low-level assault of waves and the associated movement and stresses. Moreover, sea water is very

corrosive, and materials used in the ocean must be carefully selected and maintained to avoid failure. Another substantial problem is biofouling, and any open surfaces will very quickly acquire a growth of algae and crustaceans which will impede movement and decrease efficiency. There are also substantial problems involved with working at depth in the ocean. Diving is a complex activity, and in depths exceeding 20 or 30m sophisticated techniques are required to enable divers to operate. Manned and unmanned submersible craft are also available but add another dimension to underwater work.

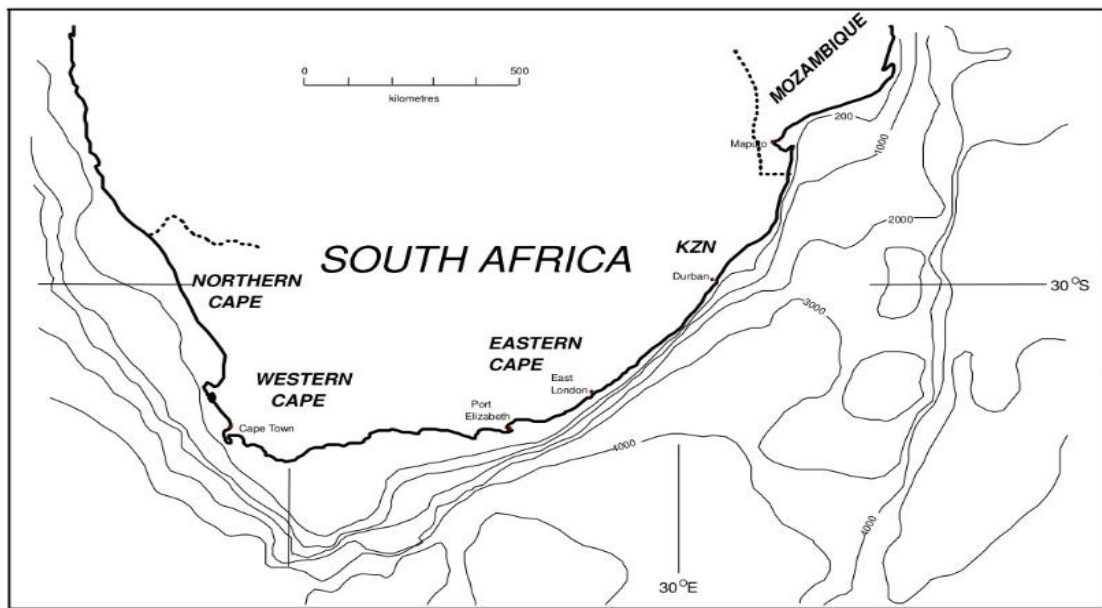


Figure 1: Bathymetry around South Africa

This description of the south-eastern shelf of Africa has covered extensive shelf and slope areas. They fall within a western boundary current region, although the presence of Madagascar serves to isolate the Mozambique Channel region. It is these intense currents flowing off. The shore of the shelf break that fornicate the corresponding coastal oceans. Particularly because of the no law shelves. Nonetheless, it must be appreciated that the subdivision of south Africa coastal ocean into this segment has been done as a convener and that there are substantial differences between the various sub regions discussed here. There are several crenulated East facing bays along the southern coast and the largest continental shelf – the Agulhas Bank – is about 270 km inland on the offshore. The key features on the shoreline are False Bay and St. Helena Bay in the west, which fig1 show above.

## 1.2. Aims and objectives.

As per history of oceans energy generation, the South Africa coastline will respond to the climate change and rise in demand of energy consumptions. However, the country has failed to produce the population energy demand due to financial barriers.

### 1.2.1. Aims

The aim of this project is to study and investigate the ocean energy in the coastline of South Africa. In conclusion the cons and frailties of the ocean's energy will be provided.

### 1.2.2. Objectives

By converting the thermal energy of the tides, waves and oceans, these technologies are starting to achieve feasibility as they are becoming potential commercial energy sources. While there are currently only a few projects, their represented technology is advancing rapidly and has enormous potential for power generation. However, the objectives of this research are as follows:

- To gather, understand and study the wave energy
- To gather, understand and study ocean current energy
- To gather, understand and study the tidal energy
- To gather, understand and study the ocean thermal energy conversion (OTEC)
- To gather, understand and study the marine winds energy
- Understand the economic valuation of ocean energy development and compare to other renewables energy for the improvement of energy demand in south Africa
- Understand all the oceans energy, identify the main problem that the country is facing with respect to renewable energy and the availability oceans energy generated, by the estimated technologies and financial barriers,

## 1.3. Problem Statement

South Africa coastal line has a potential to produce a high renewable energy that can cover a lot of cities, but the problem is the risk in the sea, water level from ocean current scale, financial barriers, and energy to manufacture the power plant and an incredible complicated life cycle in the ocean. Ocean energy makes a significant contribution to a clean and sustainable environment since renewable energy-based electricity generation is a solution for existing problems such as environmental damage, low economic growth, and human lives. In

this overview, many approaches for obtaining electricity from ocean power have been briefly examined.

#### 1.4. Research Methodology

Depending on the features of sea energy development, we may utilize the Democratic approach, the Multiple Criteria Strategy, the analytic hierarchy process, or the imprecise complete analysis approach to address varied evaluation difficulties. We integrate these two techniques by implementing the qualitative technique through interviews with experienced professionals and creating a judgement framework in the vague thorough assessment method based on the statistical results of questionnaires. We do this because the fuzzy comprehensive evaluation method will cause strong subjectivity when determining weighted coefficients, so we combine these two methods to eliminate this problem. Before we do a full evaluation of ocean energy projects, we give each parameter a weight. These weights are then put into different level groups.

#### 1.5. Research Significance

From a research point of view, wave and tidal, offer significant advantages that can boost tremendous research, with outcomes potentially applicable to other offshore activities. This is one of the main reasons, they believe, there is a vast array of turbines and wave energy converters. Indeed, wave, tidal, salinity gradients are untapped resources that offer a lot of hours of public and academic debate, in terms of their potential.

Energy generates by the ocean their stream power plants are relatively new technology, new concept and growth in a market in terms of the capacity and future investments. Most companies operate in the tidal and wave energy technology because of their significant potential of economies, benefits, massive cost reductions for a power project plants.

#### 1.6. Structural of thesis

The thesis is organised as follows:

**Chapter one:** The background of the research topic was summarized here, and the problem statement was stated clearly. The project's goal and objectives were outlined.

**Chapter two:** Examines the research's supporting literature The theory of South Africa is discussed in this chapter, as well as its capacity to be adapted to other ocean energy applications. The chapter also covers the theoretical aspects of a direct energy conversion system, including an overview of the many types of ocean energy systems and a brief discussion of the coastline system.

**Chapter three:** Selection and Comparison of technologies of ocean energies around South Africa, there are several ocean regions, each with its own set of characteristics. This section explains these characteristics in physical terms so that they can be linked to the various ocean energy sources. Technology selection and comparison.

**Chapter four:** In order to identify South Africa's most energetic coastline zone, wave data from five wave monitoring stations run by the CSIR on behalf of Port net were analysed. The country's numerous coastal regions, including the west, southwest, south, and east coastlines, were considered to be represented by the wave data from these stations.

**Chapter five:** Finding the places most suitable for wave energy conversion requires a thorough investigation of the spatial wave power distribution of the whole region. In order to do this, numerical modelling of ocean wave propagation across the aforementioned coastal region is employed. The numerical model needs deep sea wave data as input in order to mimic the transition of waves from deep water (offshore) to near-shore.

**Chapter six:** This chapter goes into depth on the design wave and water level characteristics for the proposed ShoreSWEC site. Goda's formulae were used as input, and the pressures, loads, and structural motions that resulted were assessed. The dimensions of the device construction were selected to guarantee stability under severe wave conditions.

**Chapter seven:** During this research thesis, Chapter Seven discusses other possible and attempted methodologies. It also discusses why some were discontinued. Chapter seven wraps up the research and makes recommendations for future research.

**Chapter eight:** Discussions and conclusions concerning the model are presented in the chapter's conclusion, along with important recommendations for the future development of the subject. It is also recommended what changes the facility should do to increase energy efficiency and reduce consumption in the coastline of South Africa.



## 2. Chapter Two: Literature review

### 2.1. Introduction

As per literature review, Energy generated by the ocean through stream power plants are relatively new technology, new concept and growth in a market in terms of the capacity and future investments. Indeed, wave, tidal, salinity gradients are untapped resources that offer a lot of hours of public and academic debate, in terms of their potential (Farrok *et al.*, 2020). The technology is taking a larger way path that even some of the investors are able or wish to support. Require huge financial outlays for construction of a modern power plant (Treasury, 2018). As the product of ocean energy, is to have high potential energy and a lot of natural phenomena will describe the approximate gravity of the surface in the ocean, depending to the circumstances with risk in the sea, and water level from the ocean current scale (SEA, 2017). South Africa operate most with waves energy harvesters whereas by the low frequencies and irregulars of the amplitude's energy generated by the coastline and most companies operated in the tidal and wave energy technology (Zou, 2018).

Initially it should be recognized that ocean conditions vary widely around world, and an energy extraction that can be adequate in an area will not be feasible in other. Consequently, evaluate an oceanic process and its potential to generate energy it is necessary to have a good knowledge of the ocean environment in the area. It means that each oceanographic region must be considered separately for each power source. There are several potential ocean energy sources available for South Africa coastline:

- Currents
- Tides
- Waves
- Wind
- Thermal

Note that potential sources such as osmosis and ocean biofuels are not included. In case of wind power, only the situation on the ocean itself will be considered, since there are several wind farms in operation and under construction on adjacent land. On the other hand, some of the five energy sources listed above they can be related, e.g., tides and currents but at all in this case, the primary phenomenon will be taken into consideration and, therefore, the

tidal currents will fall under the tides. The report begins with a brief review of each of the energy sources mentioned above, detailing the requirements for the extraction of exploitable energy and current situation in terms of delivery the power. Subsequently, the oceanic environment around South Africa is described in this context, and finally, the practical possibilities for each of the sources in this region are considered(Hassan and Bora, 2019).

## 2.2. Wave energy

### 2.2.1. Background

Wave energy is the potential energy in the pressure variations in water caused by waves. Because of its horizontal action, high-density energy was produced despite its low density. High-power wave generating plants would be well-suited to the coastline because of the even dispersion of wave energy there. On the other hand, a tidal power plant requires a great deal of structural engineering, severely limiting the locations at which it may be built. It's possible that even in areas where there is no wind, wave power may still be generated everywhere there is water or a cliff.

In 2008, we used over 17,000 TWh annually. Numerous WEC systems were presented as just a consequence, with the oldest known patent submitted in 1798 by Gerard and Son, with the first entire infrastructure being an Oscillating Water Column (Ocean wave energy is a potential topic for study among all sources of renewable energy. Wave power is becoming more popular as a means of producing electricity in many parts of the globe. Ocean wave energy has the capacity to generate 32,000 TWh/yr, or almost double the annual worldwide power consumption of an Ocean Wave Energy Conversion (OWEC) system that supplied a home with kilowatts in 1910. Using OWC devices is one of the most effective ways to get energy from ocean waves.

It may be situated on land or water. A new and growing interest in using the power of the waves has already been inspired by rising energy prices and the likelihood of future fossil fuel shortages. The potential power of the waves off the coast of South Africa is calculated to be around  $2.5 \times 10^8$  kilowatts. Similar results are found in this analysis, with an increase of roughly four billion kilowatts. Third-world nations that have vast coastlines but are struggling to afford rising fossil fuel prices due to industrialisation may find this resource particularly

tempting. At this time, the worldwide economic viability of using wave energy cannot be determined due to the absence of area-specific estimations of the resource. The North Atlantic, the United Kingdom, and South Africa have all had their wave energy potentials determined. The goal of this research is to figure out how strong waves are on all of South Africa's coasts where people live(Martínez, Silva and Garcia, 2021).

Inherent, extremely wide variation in output power at very low frequencies is a feature of Wave Energy Converters (WEC) due to the time of ocean waves, which is typically around 10 seconds(de Vos, Vichi and Rautenbach, 2021). Due to the need for continual cyclic charging and discharging of data storage, the Extremely System for Energy Storage (SES) has been shown to be a viable option for resolving variation concerns, especially in WECs.(Lieber, 2021)(Singh Randhawa, 2015). We need a power electronics converter system to link the WEC to the power grid in addition to the energy storage capacity of the WEC(de Vos, Vichi and Rautenbach, 2021). Significant breakthroughs have been achieved in systems capable of turning wave kinetic energy into electrical energy in a more efficient and cost-effective manner as we attempt to reduce global fossil fuel dependence. Furthermore, as these technologies' commercialization progresses, many resources assessment studies have been conducted in the last decade.

### 2.2.2. Effective wave energy conversion

There is a wide range of wave energy converters on the market, each with its own size and efficiency profile (WEC). Most WECs are categorized by the part of the wave that is used to generate electricity. The most common types of WECs include terminators, attenuators, point absorbers, and overtopping devices.

- In order to limit the further spread of a wave, terminator WECs may absorb its energy. These WECs are often located near coast since waves end there.
- Equalizer wave energy converters (WECs) are floating on the edge of the water or are just partially submerged. Typically, they'll feature a hinge mechanism and a body part that can pivot separately on the hinge. When a wave passes through an attenuator, some of its energy is stored, and the wave may then move farther along the ocean's surface. Overcoming Devices, Point Absorbent Materials, and Attenuator Whole-Electric Circuits.

- If a wave's energy is taken up by a stationary physical system that depends on changes in pressure and/or altitude at the water's surface, the wave won't be affected and will keep moving across the ocean.
- Capturing water as it flows over a dividing line, then using the resulting hydrostatic pressure to power an electrical generator.

### 2.2.3. Calculations

$P$  (kW/m), or power per unit wave crest length, is a common measure of wave energy resource that is calculated from measured spectra using the formula.

$$P = \frac{\rho g^2}{4\pi} m_1 \quad (1)$$

where  $g$  is the acceleration due to gravity (9.81 m/s) and  $\rho$  is the density of sea water (1025 kg/m<sup>3</sup>). More generally, Equation 1 is expressed in terms of  $H_{m0}$  and  $T_E$ , yielding

$$P = 0.49 H_{m0}^2 T_E \quad (2)$$

Previous research (Ghosh and Prelas, 2011) has shown that a small number of extremely high sea states caused by strong storms can contribute disproportionately to the annual energy experienced at a location. However, under these extreme conditions, a WEC's performance would be drastically decreased due to efficiency losses, or even zero as the device entered survival mode.  $P_{exp}$ , the concept of exploitable power, was developed in to account for this.  $P_{exp}$  is stated mathematically in Equation 3 as four times the average incident wave power.

$$P_{exp} = 4 \frac{\sum_{i=1}^N P_i}{N} \quad (3)$$

Any power above the  $P_{exp}$  is considered redundant in highly energetic sea states and is discounted. While the value of  $P_{exp}$  supplied by Equation 3 is rather arbitrary, it nevertheless serves as a valuable tool for determining what range of sea states should be considered relevant for wave power capture.

$$\Delta E = \rho \frac{\partial \phi}{\partial t} V = \rho \frac{\partial \phi}{\partial t} \nabla \phi \quad (4)$$

Mainly, the wave's horizontal presentation as it comes in at a typical angle to the damaged coastline is what's taken into account while collecting the wave's energy as it travels inland (Maristany *et al.*, 2012). The rate of change in energy per unit area per unit time perpendicular to the direction of flow is known as the energy flux. Multiplying the energy density by the particle speeds yields the energy flow (see Eq. 4 the Wave Energy Flux) (Maristany *et al.*, 2012).

$$E = \frac{\rho g a^2 c_g}{2} i \quad (5)$$

In Eq. 5, the mean wave energy flow is shown by expressing the velocity potential in terms of wave height, water depth, horizontal distance over a certain amount of time, and wave length, and then integrating this over the wave period and the water depth (Maristany *et al.*, 2012).

## 2.3. Ocean current energy

### 2.3.1. Background

Oceans current energy has become an important road to developing renewable energy as a broad resource and sustainable energy. Most studies on current energy at sea currently centred on the creation of different types of generators and blades to effectively exploit currents and work has been lacking on how to use current streams across a wide scope (Schumann, 2014).

This section deals with ocean currents but excludes those due to tides; these are treated separately in §1.2. However, the turbines that are in use and in the development, process is obviously not limited to forms of ocean current. The Agulhas Current, as previously indicated, is the only possible South-African power source to be used. Eskom has acknowledged this potential, and current meter are used on various sites on the continental shelf and slope off the eastern coast for five years from 2005 to 2010. See Figure 2.

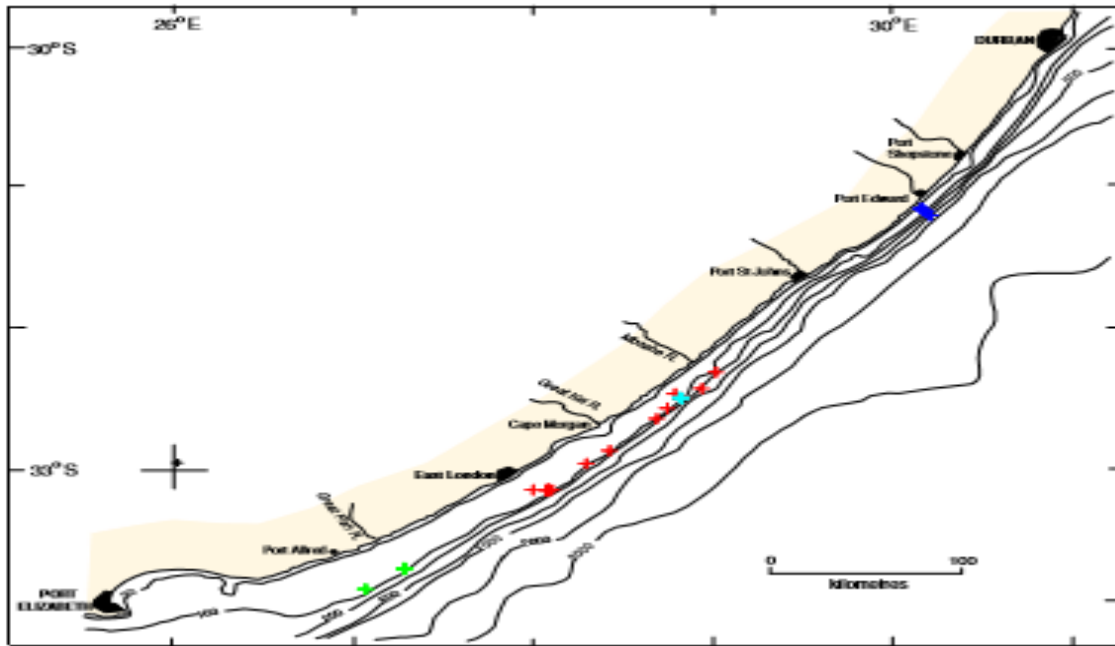


Figure 2: The current meter deployments' approximate locations.

On a global scale, long-term wind systems are the result of thermal energy from the sun, and in turn, established the current structures on the scale of the ocean basin. Of importance are trade winds mainly within about 20° from the equator and more towards the pole where the western wind belts are north and south of 30°. These winds drive clockwise turns in the ocean basins of the northern hemisphere and anti-clockwise it travels in the ocean basins of the southern hemisphere (Blake, 2010). However, how because of the earth's rotation, the currents to the west are forced to flow like as close as possible to adjacent continents. This results in the so-called western limit currents, the most famous being the Gulf Stream that flows north-east along the east coast of south Africa (Schumann, 2015).

The south Africa and other countries are very interested in the possibility of exploiting ocean currents as a viable fossil-fuel alternative for energy generation in certain parts of the world. Devices can be simplified and operated more successfully in tidal regions due to the continuous flow directions without reversals (Chakraborty *et al.*, 2021). However, because generators are built to use this feature, it's critical to know when and to what extent direction shifts may occur, even during extreme weather. Successive underwater generating "farms" may be practical and economically effective in the near future, thanks to advances in offshore technologies, support vessels, generators, and procedures (Hsu *et al.*, 2008). Despite advances in technology, knowledge of the spatial and temporal diversity within these currents, notably

reversals, is still limited. The energy flow that has so much potential for power generation has resisted careful observations since the 1880s, and the problem persists today.

### 2.3.2. Observation

The measurements were taken at a depth of 32 meters north of Kuchinoshima Island at 30° 03' 16" N, 129° 51' 48" E. Nortek's Signature 500 ADCP and Vector ADV measurement equipment were bottom-mounted and separated by a distance equal to two times the water depth to reduce the likelihood of interference from other acoustic signals. The 15th and 16th of January this year saw just around 22.5 hours of observations due to bad weather.

#### 2.3.2.1. *Acoustic Doppler Velocity Profiler (ADCP) data*

The Signature 500 ADCP was utilized to collect data at a sample rate of 4 Hz from 1 m cells over the entire 32 m water column. Nortek, the Signature 500's manufacturer, claims that their product has an estimated standard deviation of 7.34 cm/s for horizontal velocity when sampled at 4Hz. Figure 4 provides an example of raw data(Imamura, Takagi and Nagaya, 2019). The raw data must go through a number of transformations before analysis can begin. Anomaly spikes and other erroneous data are eliminated(Johnson and Fourie, 2012)(Imamura, Takagi and Nagaya, 2019). Consideration is given to the Signal to Noise Ratio (SNR). As can be observed in Fig.5, the high quality of the water at Kuchinoshima might lead to a low SNR when using ADCP instruments, which rely on the reflection of acoustic signals from suspended particles in the water. Correlation between the acoustic signal beams also affects the quality of the data. Figure 6 shows that between the time domain and the water column, the observed connection is rather strong(Imamura, Takagi and Nagaya, 2019).

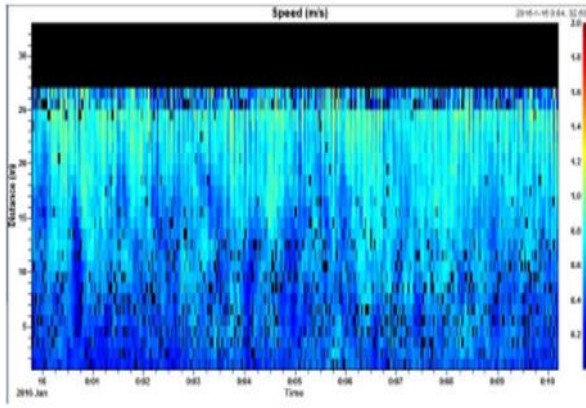


Figure 3: Ten minute sample ADCP speed data

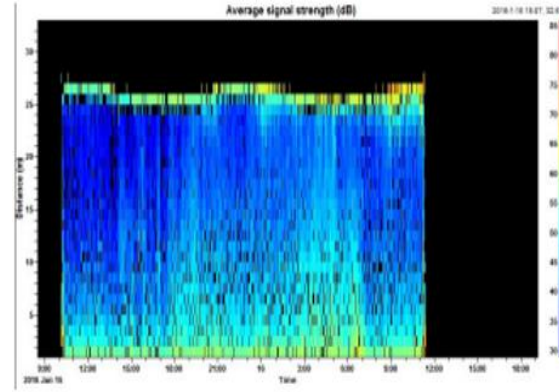


Figure 4: The ADCP observation average signal strength reflects the high water clarity

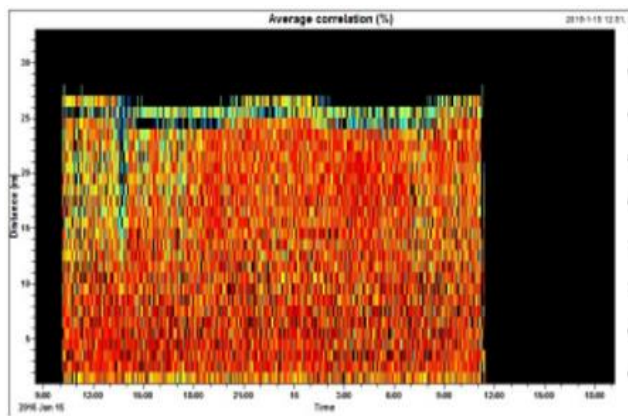


Figure 5: Average correlation (%) for the ADCP observation

### 2.3.2.2. Acoustic Doppler Velocimetry (ADV) data

A second Nortek sensor, the Vector ADV, was used to calculate current speed in the deepest parts of the river. The Vector is a downward-facing device that is installed on the seabed and collects data at a sampling rate of 16 Hz at a height of one meter above the ground. In the next section, we'll talk about spectral analysis, which is based on the ADV data (Imamura, Takagi and Nagaya, 2019).

## 2.4. Tidal energy

### 2.4.1. Background

Tides are the up-and-down movement of the sea surface that happens on a very regular basis due to the astronomical motions of the earth, sun, and moon. Potential energy created by



fluctuating sea levels is known as tidal energy. The tidal current is a horizontal water movement whose energy is derived from the kinetic energy of water flow.

The energy of tidal currents is not affected by the seasons but rather by the twice-daily small changes in tidal level and the twice-weekly larger variations in tidal level. In the same way that the tidal range changes every seven hours and fifteen minutes, the tidal current also changes on a sine-based schedule. When the tide current is moving faster than 2 m/s, the building will be worth what it is really worth.

Tides in the ocean occur as a result of the orbital movements of the Sun / Earth / Moon system. The details of the various orbits and the resulting forces are described in various textbooks and will not be addressed here. A brief summary of what is relevant the results are shown below:

- Although the mass of the Sun is much more than that of the Moon, it is around 360 times farther away from Earth, and consequently the tidal production force of the Sun is about 0.46 that of the Moon.
- Complex orbits, involving aspects such as the declinations of the Sun and the Moon and Elliptical orbits produce many harmonic components, each of which contribute to the tide at any time and place.
- The ocean's response to tidal forcing depends on bathymetry and morphology. And shape of ocean basins. In general, tides propagate as Kelvin waves advance in an anti-clockwise around an immobile amphiprotic point to the north hemisphere. In the southern hemisphere, the spread is clockwise.

Each ocean basin responds differently to the forcing of the tides. The resulting movements are complex, with several amphiprotic systems interacting. Figure 1 shows the M2 tide in the English Channel that propagates like a Kelvin wave heading north-east. It's important Keep in mind that the peak of the wave takes about 6 hours to travel the length of the channel, which means that it is low tide on one end and high tide on the other(Johnson and Fourie, 2012).

#### 2.4.2. [Methods of tide generations](#)

Basically, there are two ways in which the tide is generated: The tidal current generator directly uses the kinetic energy of moving water to generate energy. Turbines, like wind turbines that use the wind to power turbines. Some tides the generators can be integrated

into existing bridge structures. The tidal dams exploit the amplitude of the tides. During the flood tide, the entrance is conveyed A large basin behind the barrier(Richardson, 2019). At low tide, water is released through the turbines create electricity using generators. There are several other tidal power plants operating in various parts of the world, the Much smaller than La Ranke. However, in 2011 the largest operating station, the tidal power plant of Lake Schwa in South Korea has been opened. There are several proposed new bombing stations, including one in the Severn estuary, but associated Environmental problems are proving to be a serious disadvantage. However, there are currently no large operational turbine stations located directly in the tidal flows. Some are at an advanced planning stage.

## 2.5. Ocean thermal energy conversion

### 2.5.1. Background

The term "Ocean Thermal Energy," or "OTE," refers to the process of harnessing the heat differential between the ocean's surface and its depths to power a heat engine.(Griekspoor, 1981). OTEC often employs the Rankine cycle with a low-pressure turbine since this is the most widely utilized thermal cycle for such applications. There are three possible types of systems: open circuit, closed circuit, and a hybrid that combines the two. The open cycle engine uses hot sea water directly to generate electricity and steam Sea water is the working fluid. Pumping hot sea water into a low-pressure container bubbles and the expanding steam pushes a low-pressure turbine connected to an electrical system generator(Schumann, 2017). The vapour is almost fresh water and condenses again into a liquid on display the cold and deep water of the sea Closed loop systems use a low boiling point working fluid to rotate the turbine(Treasury, 2018). Warm surface seawater is pumped through a heat exchanger where the low boiling points the fluid vaporizes, and the expanding steam makes the turbo generator turn. The deep cold sea water is pumped through a second heat exchanger and condenses the liquid vapour again a liquid, which is then recycled through the system(Magagna, Monfardini and Uihlein, 2018).

The concepts involved in the use of OTE have been known for a long time, proposed for the first time by the French physicist Jacques D'Arsonval in 1881. In 1930 Professor G Claude experimented with the production of OTE energy in the bay of Matanzas, Cuba, and they managed to generate 22 kilowatts for 10 days, using a real thermal difference of 14 °C in sea water. Claude continued with his experiments on the Brazilian coast, and in 1940 he started

a project in front of Abidjan, in Ivory Coast this was to generate 15 MW of electricity using a 4 km long pumping tube Cold water from a depth of 430m. However, this was abandoned in the 1950s when I was older. Quantities of oil have become available cheaply and therefore have denied economic viability project.

However, in the early 1980s, funding for ocean energy research and development in the United States UU. He suffered badly cuts, mainly due to the change in Carter's energy R&D philosophy Administration (1977-1981) to the Reagan and Bush administrations. More recently there the interest was renewed at the federal level, with the final design phase of a 10 MW closed cycle The OTEC pilot system will begin operating in Hawaii in the 2012-2013 period.

Additional benefits of using OTE for electricity generation are base load power it works 24 hours a day, 7 days a week and there are several possibilities products including freshwater production, Mari cultural, air conditioning and chilled land agriculture. The specific disadvantages are mainly related to the practical application of the process in the ocean, i.e. the deployment of large diameter pipes of over one kilometre want access to deep and cold water, while gases also come out of the solution as deep water it approaches the surface and the pressure decreases.

#### 2.5.2. An OTE Plant's Location and Potential Impacts

The continental shelf off the shore at the OTE location is relatively small, as seen by the isobaths in Figure 1. A multitude of canyons, running from the continental shelf and down the slope into the deep, have been discovered in the area. The strong Agulhas Current makes anchoring and maintaining the position of a floating OTE plant problematic. Furthermore, an OTE plant must be as close to the land as feasible while still being able to reach deeper, colder waters, which implies that a shore or shelf-based plant off northern KZN is a must; as a result, these are the only possibilities that will be evaluated here(Committee and Engineering, 2012).

The canyons provide access to deeper water closer to the coast. In addition, depending on the option selected, a canyon could provide a conduit for a pipe to reach the colder bottom water, providing protection from strong currents associated with the Agulhas Current. The dynamic upwards sloping of the isotherms close to the coast also means that deep water should be accessed as close to the coast as possible. At this stage it appears that using one of

the canyons for the deep-water pipeline will be the most appropriate technique for an OTE plant situated at the shore or near the shelf break(Agarwal *et al.*, 2022).

The proposed OTE location, however, is located offshore of the iSimangaliso Wetlands Park, which was designated as a World Heritage Site in 1999. A Marine Protected Area (MPA) is defined as a stretch of coastline reaching 3 nautical miles (5.56 kilometers) out to sea from Cape Vidal (approximately 25 kilometers south of Leven Point) to north of Kosi Bay (70 kilometers north of Sodwana Bay) and extending 3 nautical miles (5.56 kilometers) out to sea. This means that the development of an OTE in a land-based or near-shore location will require special clearance. As a result, the potential OTE plant detailed here is located outside of the MPA(Hassan and Bora, 2019)(Farrok *et al.*, 2020).

It's also worth noting that the Agulhas Current core, which is often located near the shelf breach, has the highest sea surface temperatures. The fall in temperature as you get closer to the seaside argues against putting the OTE plant there. At this time, the Wright and White Sands canyons, located just north of Sodwana Bay, appear to be the finest locations for an OTE plant. These locations are on the outskirts of the iSimangaliso Wetlands Park's marine reserve, while the marine sanctuary's more restricted territory lies to the south.

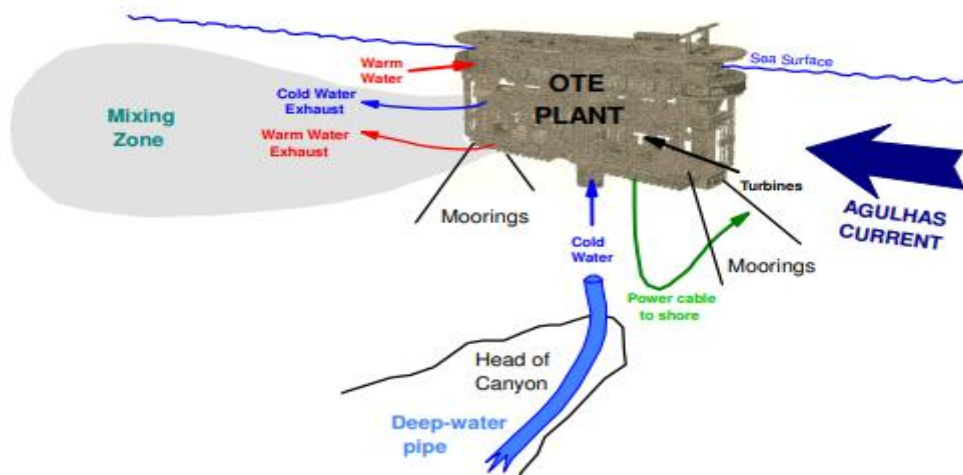


Figure 6:An OTE facility near the coast of Wright Canyon is depicted schematically (courtesy of Sea Solar Power, Jacobus, PA, USA)

Figure 6 shows a typical OTE plant. It's vital to remember that the majority of the OTE plant is below the water's surface. This decreases the potential for extreme weather and sea conditions to cause damage and makes it much safer. Furthermore, because the surface

expression is modest, it has little aesthetic influence. The cold water outflow is the only thing that has a negative impact on the environment. According to calculations, the water emitted by the OTE plant will be roughly 7 degrees Celsius cooler than the surrounding water, despite the fact that natural temperature variability is likely to be more than 7 degrees Celsius, with upwelling cells occurring on occasion closer to the shore. The plant's design, however, will result in a limited mid-water mixing zone due to the locations of the cold water (sinking) and warm water (rising) exhausts (Richardson, 2019). The major position of this mixing zone will most likely be downstream of the Agulhas Current's flow. The area's physical oceanography is quite well understood (e.g., Schumann 1988, 1998), and there are no known processes that might push cold water over inshore reefs before mixing has neutralized any negative impacts. It's worth noting that the cold water exhaust water is likely to have high nutrition levels as well.

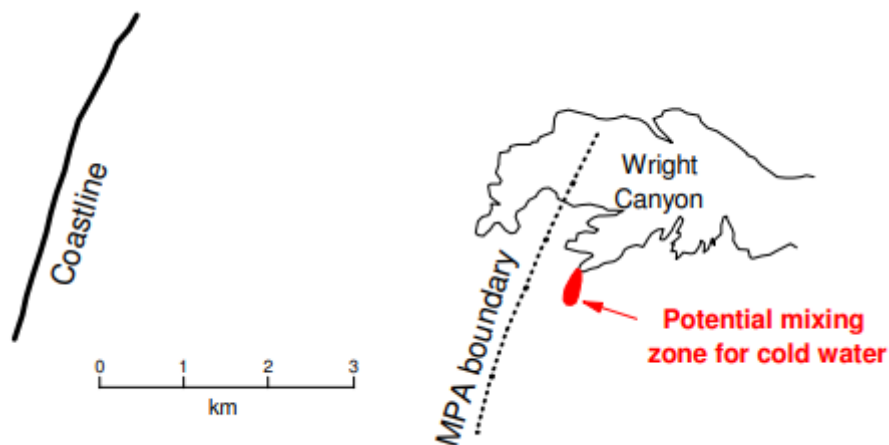


Figure 7: An OTE plant's relative position and influence

Figure 7 depicts the operation's scale in relation to the coastline, the head of Wright Canyon, and the offshore location of the Marine Protected Area (MPA) associated with the iSimangaliso Wetlands Park. Apart from providing much-needed electrical power to the region, the desalinated water produced as part of the electricity-generating process can also be used. A 100 MW OTE plant can desalinate approximately 100 000 m<sup>3</sup> of water per day (Terao and Sakagami, 2014). This volume of fresh water might go a long way toward alleviating the effects of the region's droughts. Furthermore, it may be able to use nutrients from deep water in fish cages, for example.

These findings suggest that OTE could be a viable source of renewable ocean energy. More exact and reliable data is needed to establish whether the temperature differentials are large enough to warrant serious consideration of an OTE device. This will entail placing vertical arrays of temperature sensors in strategic locations, such as the Wright Canyon mentioned above. At the same time, current meters should be installed since complicated current structures may form in the canyon as a result of Agulhas Current offshoots(Zou, 2018). These could also be used to examine the canyon's potential for slumping. The wind-index is determined by considering the following elements. Wind speed measurements from the SSM/I was used to calculate an offshore wind farm relevant wind index, which was then extended to 80m above sea level using a logarithmic profile and a shear of 0.1. Since this is the case, a scaling factor of 1.23 was arrived at.

## 2.6. Marine winds energy

### 2.6.1. Background

The wind has long been recognized as a usable energy source and the use of windmills has been widespread in many parts of the world for centuries, while sailing boats have used wind energy For thousands of years More large wind farms and wind energy have been created more recently Generation now forms an increasing percentage of the energy mix of many countries(Baumgardner, 2016). Wind of the world generation capacity quadrupled between 2000 and 2006, doubling every three years; at the end of 2012, the global capacity of wind turbines was 282 GW.

There is a growing trend to harvest energy from sea breezes, which are often stronger than land winds. There is less turbulence and less wind-shear, and the sea regions are not immediately impacted because of the shape of the soil(DFFE, 2021). There are also enormous continuous areas accessible, making them ideal for major projects. In addition to reducing fatigue loads on turbines and allowing for shorter towers, this improves the efficiency with which turbines gather energy. Furthermore, land regions are more likely to face criticism for environmental reasons than wind turbine placement for energy extraction(Wecs, Archipelago and Girard, 2009).

The impact of the wind on the high seas Bird farms are generally considered to be the most important environmental impact. However, addressing this is the very important

disadvantage of additional capital investment. Necessary for offshore wind farms. Marine foundations are more expensive, the installation procedures are also more expensive, with limited access during construction due to weather conditions. In addition, there is usually a more expensive one integration into the electricity grid and in case of limited access during operations e maintenance can lead to a reduction in turbine availability and therefore a reduction in performance

### 2.6.2. Estimation of wind resources

Though indicative of the wind environment, the average wind speed alone is insufficient for estimating the potential wind resource. There is a nonlinear connection between the speed of the wind and the amount of energy generated by a wind turbine, so it may be used at a wide range of wind speeds. When winds are weak, a turbine won't spin (e.g., less than 4 m/s). Specifically, for winds between 4 and 13 m/s, the potential power is proportional to the cube of the wind speed. When the wind speed is between 13 m/s and 24 m/s, the wind turbine keeps producing its full rated power. If the wind speed goes above 24 m/s, the wind turbine shuts down to prevent any structural damage (Hasager, Astrup and Nielsen, 2007).

Using the average wind speed at the rotor's center, the power curve depicts the relationship between the two variables (at hub height). Variations in wind speed over the course of a few seconds, minutes, hours, days, months, seasons, and decades are notable on any time scale. A simple method for estimating the available wind power in a given area is to fit the Weibull function to a histogram of the time series of wind speeds. This involves determining the shape (k) and scale (A) of the distribution (Hasager, Astrup and Nielsen, 2007). The potential power output for a given wind turbine may then be estimated by combining the power curve and Weibull parameters, as is done in programs like WAsP (Wind Atlas and Analysis Program). Because one wind turbine upwind of another would have a shadowing effect (wake) downstream, resulting in decreased output power from a turbine in the wake due to the lower mean wind speed, the wind direction is crucial for the architecture of a wind farm (and higher turbulence intensity) (Neil Habig, 2004).

The nearest surface current grid point with at least 70% temporal coverage during the research period was utilized to compare with the wind measurements. First, the surface current data was derived using the least squares approach, which factored in the five primary

aspects of the study area (M2, S2, N2, K1, and O1)(Neil Habig, 2004). Then, a 30-hour low-pass filter was applied to the currents. For the east-west velocity  $u$ , see Figure 2, and for the north-south different velocities, see Figure 3.

## 2.7. Economic valuation of ocean energy

### 2.7.1. Background

Chinese economic growth in recent years has allowed the country to overtake the Us as the world's second biggest user of energy and a contributor to greenhouse gas emissions (SEA, 2017). It's important to remember that China's CO<sub>2</sub> emissions almost quadrupled between 2002 and 2007, and that this rapid growth has led to widespread anticipation that China would soon replace the United States as the world's greatest CO<sub>2</sub> emitter(Chen *et al.*, 2022). There will be increasing calls for China to cut its carbon output from the international community. To assure long-term economic and social growth, the South African government aimed high in its 11th Five-Year National Economic and Social Development Plan, calling for a 20% improvement in energy efficiency and a 10% reduction in pollution by 2010. Because of the country's size, South Africa's economic growth is not uniform throughout the country. This is clear not only from the wide range of social and economic progress around the world, but also from the huge differences in how much energy is used and how much carbon dioxide is released(Chen *et al.*, 2022).

Conflicts over energy usage, economic growth, and CO<sub>2</sub> emissions are on the rise with the expansion of the global economy. Studying the spatial-temporal interaction between the economy, the energy sector, and the environment (3E system) is essential for China's efforts to lower energy consumption and carbon dioxide emissions. Few studies have investigated how rising GDP affects energy use and greenhouse gas emissions. One of our major contributions, then, is this. Traditional statistical methods may be used to resolve such worries if there is sufficient data for statistical significance. However, provincial data on energy use and carbon dioxide emissions in South Africa is hard to come by. Despite the lack of data, grey relational analysis (GRA) can be used to analyse correlations and performance of the 3E system at the provincial level(Imamura, Takagi and Nagaya, 2019). Doing this kind of study would aid our understanding of the interdependencies between the systems in Province 3E. We anticipate that our study's findings will have policy implications for the



province in the areas of energy saving and emission reduction. Deng's (1982) grey system theory includes grey relational analysis (GRA), which is helpful for addressing issues with many components and variables with complicated interrelationships (Solution, Machine and Algorithm, 2019).

## 2.7.2. Methodology and Data sources

### 2.7.2.1. Methodology

In relational geometry, grey relational analysis-based calculations look at how time series and data are related to each other in space (Agarwal *et al.*, 2022). To rephrase, the partial correlation class in a particular system indicates the relative variances between the reference sequence and the compared sequences (Chen *et al.*, 2022). If there is little fluctuation in relative terms between the two-time series as they evolve, then the correlation grade is high, and vice versa. There are two parts to a GRA. The relative degree is the first factor to consider since it quantifies how much the sequences under consideration affect the standard sequence. The comparative polarities of the sequences under comparison to the reference sequence establishes the direction of the effect (+ or-).

Let  $X$  be the grey relational set,  $X_0 = (x_0(1), x_0(2), \dots, x_0(n)) \in X$  represents the reference and  $X_i = (x_i(1), x_i(2), \dots, x_i(n)) \in X$  ( $i = 1, 2, \dots, m$ )

represents the sequences that were compared in this case,  $m$  denotes the number of compared sequences and  $n$  denotes the length of time sequences.

Let

$$\Delta_{oi}(k) = [x_0(k) - x_i(k)] \quad (6)$$

$$\Delta_{min} = \min_i \max_k [x_0(k) - x_i(k)] \quad (7)$$

$$\Delta_{max} = \min_i \max_k [x_0(k) - x_i(k)] \quad (8)$$

At time point  $k$ , the grey relational coefficient of compared sequences  $x_i$  to reference sequence  $x_0$  is defined as follows:

$$\xi_{oi}(k) = \frac{\Delta_{min} + \rho \Delta_{max}}{\Delta_{oi}(k) + \rho \Delta_{max}} \quad (9)$$

where  $\rho$  is the distinguishing coefficient, commonly [0,1], that is used to alter the difference of the relational coefficient. We used a value of 0.5 for further investigation in this study. If we assume that each point in a sequence is equally important,

we can calculate the grey relational grade between reference and compared sequences  $X_i$  by averaging relational coefficients at all-time points:

#### 2.7.2.2. Data sources

When analysing the effectiveness of provincial 3E systems in South Africa, researchers use the grey relational approach outlined above to learn more about the interconnections between energy, the environment, and the economy (Chen *et al.*, 2022). The data used in the analysis spans from 1998 to 2007, since it is readily available and somewhat stable across that time period. The South Africa Statistical Yearbook (CSY) (SSB, 1999-2012) and the South Africa Energy Statistics Year (CESY) provide information on GDP, industrial structure (primary, secondary, and tertiary sectors), and energy consumption by province (SSB, 1997-1999, 2000-2002, 2003-2008).

## 2.8. Conclusion

As for the conclusion to commercialise and industrialise ocean energy development technologies, all parties, including the government, investors, engineers, and technicians, must work together to resolve economic concerns. The majority of ocean energy development technologies have yet to be commercialised. This is because of the properties of ocean energy: When compared to traditional energy sources, they are relatively unstable and have a low energy density. As a result, when compared to traditional resources, ocean energy has a price disadvantage. However, as the scale of development expands, ocean energy begins to show clear advantages. As illustrated in Fig. 1, the generation cost of ocean energy will be even lower than that of a coal-fired plant, indicating robust price competition. Furthermore, because the operating costs of ocean energy utilisation projects are generally low, ocean energy will have a bright future if its stability is improved. Now is an excellent time to invest in ocean energy. Ocean energy will grow in the future, thanks to government backing

and the efforts of all parties. It's logical to suppose that today's wind energy will be tomorrow's ocean energy.

### 3. Chapter Three: Selection and Comparison of technologies

#### 3.1. Background

There are various ocean regions around South Africa, each with its own set of characteristics. These features are outlined in physical terms in this section in order to relate them to the many potential ocean energy sources.

Ocean currents are a significant distinguishing characteristic, with the Agulhas Current being the dominant oceanic feature on the east coast. The Agulhas is one of the greatest western border currents, with an average volume flow of roughly  $70 \times 10^6 \text{ m}^3 / \text{s}$  (Schumann, 1998; Lutjeharms, 2006). With a large migration of warm tropical and subtropical seas being moved southward, it plays a significant role in the global heat budget. The condition is depicted in Figure 8, where sea surface temperatures (SSTs) clearly indicate the Agulhas Current as a narrow, fast-moving stream travelling down the shoreline. Despite the fact that the photograph was shot in the middle of winter, sea temperatures off northern KwaZulu-Natal (KZN) were still around 24 degrees Celsius. The gradual cooling to the south is clearly visible.

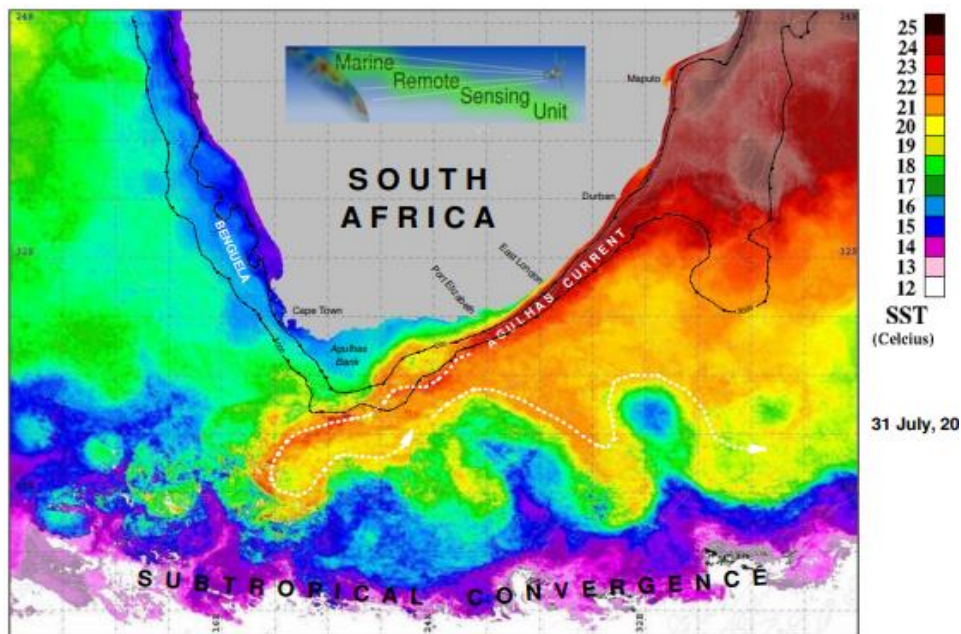


Figure 8: composite false colour satellite image of sea surface temperatures on the provided scale, collected on July 31, 2020 (with thanks to the Marine Remote Sensing Unit).

The Agulhas Current runs south-westward, with the core running parallel to the bathymetry on average. There are considerable offshore gradients in current speed and temperature, especially at the surface, on the coastal side, i.e. both speeds and temperatures increase with distance offshore (Pearce, 1977). The current's core is usually found at the shelf break, with peak speeds in excess of 2 m/s; speeds diminish more gradually beyond the core. The flow reaches depths of more than 2000 m and rapidly diminishes with depth.

Water temperatures drop as you go deeper, but there's little evidence of a strong thermocline structure. The isotherms on the inshore side slope upwards as a result of the Current's dynamics. Figure 9 shows a part of the Port Edward offshore that demonstrates these qualities. In Appendix B, we provide a comprehensive history of wave metering in that country. In most cases, wave information was gathered on a case-by-case basis, with an emphasis on satisfying the needs of coastal engineers (Meyer *et al.*, 2013). Real-time wind and wave data was in high demand as South Africa's marine industry expanded, necessitating automation of data collecting to ensure an effective and economical system. When strong waves are predicted, authorities in charge of offshore constructions (such the MossGas FA Platform) and South Africa's key ports (the Transnet National Ports Authority) need truthful data on these level zones to take the necessary measures (Meyer *et al.*, 2013).

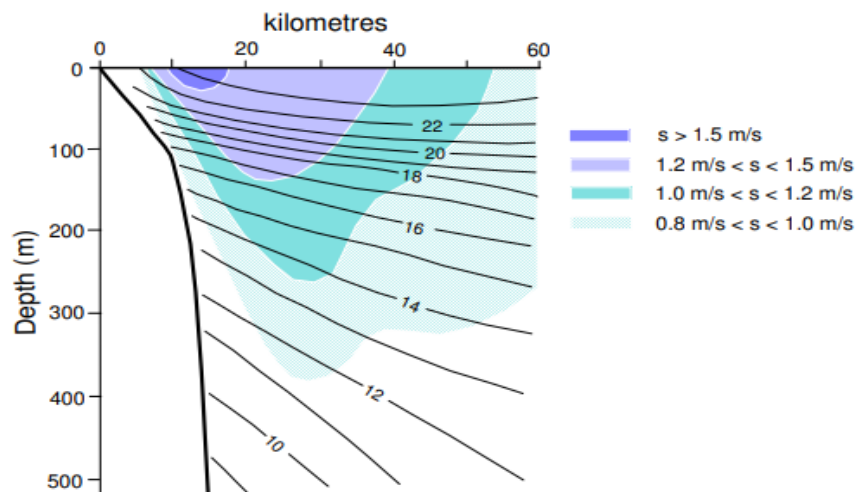


Figure 9: The temperature structure ( $^{\circ}\text{C}$ ) and accompanying currents with speed's' are shown in an offshore region at Port Edward (adapted from Pearce, 2019).

As low pressure systems in the Indian and South Atlantic move eastward, they expose Africa's south-western coast to a vigorous wave regime. These depressions, which are often

accompanied by cold fronts and wind fields, are the primary source of ocean wave energy that reaches the south-western African coastline. The western Indian Ocean's tropical cyclones provide a significant amount of wave energy to the south and east African coasts(Meyer *et al.*, 2013). Wave data recorded at stations around the South African coastline may be analysed to provide information about the coast's dominant wave conditions and the region's highest wave power reserve (see Fig. 1)(Meyer *et al.*, 2013). The predicted average, 90% likelihood of exceedance, and 5% probability of exceedance of wave power on the South African coast are shown in Table 1 for significant wave height ( $H_s$ ), peak period ( $T_p$ ), and wave power ( $P$ , kW per meter wave crest).

Table 1: Wave height, period, and power are statistical parameters that are averaged over a year.

Recording station	Ave $H_s(m)$	2:10 year $H_s(m)$	Ave $T_s(s)$	Ave $P(kw/m)$	9% P	89 % P
Port Nolloth	1.9	10.2	11	17	83	8
Slangkop	3.3	9.5	11	28	99	11
Cape Point	3.2	12.3	11	28	107	10
FA platform	3.7	9.9	8	25	88	9
Durban	2.1	8.2	9	15	44	6

A maximum annual average maximum output of roughly 40 kW/m was measured at the Slangkop and Cape Point stations, which is consistent with the relatively high energy intensity of the southern African wave regime, as shown in Table 1. This and other comparisons suggest that the Southwest coast has the greatest wave power resource because of its proximity to the storm producing zone in the lower latitudes(Meyer *et al.*, 2013). South Africa has a large wave energy resource that may be converted into usable forms of energy. The mean annual average deep sea wave power is around 42 kW/m, decreasing to 39 kW/m near the coast. In the past, Stellenbosch University developed a game-changing, homegrown WEC called the SWEC to efficiently convert ocean energy in typical South African wave conditions(Meyer *et al.*, 2013).

The strong turnout at the first-ever ocean energy workshop demonstrates South Africa's growing interest in wave energy development.

Major worldwide wave energy technology companies have taken note of the potential for wave energy development in southern Africa, with a number of projects planned for the southwest and south coastlines. Pelamis Wave Power Ltd. of Scotland has chosen locations on the southern Cape coast of South Africa to place its Pelamis attenuator WEC device after an initial review of available resources. Finavera Renewables conducted an initial feasibility assessment on the use of Aquabuoy devices in the Indian Ocean off the southwest coast of South Africa in 2006. Oceanlinx, an Australian company, is building a 15 MW wave farm off the coast of Namibia, which is another example of a wave energy project(Meyer *et al.*, 2013).

### 3.2. Comparison of technologies

Even though we have many ideas for harnessing the energy of ocean waves and tides, feasibility remains a challenge. To be cost-effective in the energy generation industry, the turbine must create a large amount of energy. Despite the fact that the motion of tides and waves in the world's oceans contains a massive quantity of energy, there are only a few sites with enough ocean energy to justify the installation of energy devices(Pereiras, Valdez and Castro, 2014).

Another major impediment to the production of energy from seas is the ocean itself. The ideal locations for the installation of energy turbines are in areas where there are more turbulent currents. Many new technologies have been ripped apart when they are tested at sea. As a result, ocean energy turbines should be able to withstand the harshest conditions. This is accomplished by comprehensive studies to ensure mandatory sustainability, as well as major investments in structures and materials capable of bearing high loads. Figure 1 depicts a map of South Africa with average wave energy throughout coastal locations throughout the country(Sahed and Ismail Alnaimi, 2014). It is clear from this card that there are relatively few areas in South Africa where energy systems with current technologies can be installed. Waves can only be used as a source of energy in select portions of South Africa's coastline due to current technological limitations.



Figure 10: The South African coastline's average wave energy (from van Niekerk, 2012)

The CSIR operates wave measuring stations at Port Nolloth, Slangkop, Cape Point, Mossos FA Platform, and Durban along the South African coast (Joubert, 2013a). The mean wave energy were calculated using these measurements (Fairhurst, 2015).

Figure 9 shows the results, which reveal that there is significant wave energy along parts of South Africa's coast. When averaged over a year, the strength of the wave energy resource ranges from 15 to 40 kW/m, with the west and south coasts having the largest resource. Wave energy dramatically decreases as one travels north along both the east and west coasts.

The amount of wave energy available ranges from less than 10 kW/m in the summer to more than 100 kW/m during a winter storm. The threshold for a commercially viable wave energy resource is set at 30 kW/m of average yearly wave energy (Elizabeth, 2017).

The way waves approach the beach is affected by wave properties such as period, length, and direction. In order to select the ideal sites for wave energy converters, a comprehensive investigation of specific portions of coastline is required to establish where wave power is focused. Furthermore, the ideal sites for such devices will be determined by the technology employed.

The most crucial parameters for describing a simple harmonic wave are its wavelength  $L$  (the horizontal distance between two successive wave troughs or crests), its period  $T$  (the time it takes a wavelength to pass a given point), its wave height  $H$  (the vertical distance between the trough and the succeeding crest), and its water depth  $d$  (the vertical distance from the seafloor to still water level (SWL)) (Joubert, 2013a). All of these characteristics are shown for a linear wave as a function of phase in Figure 11.



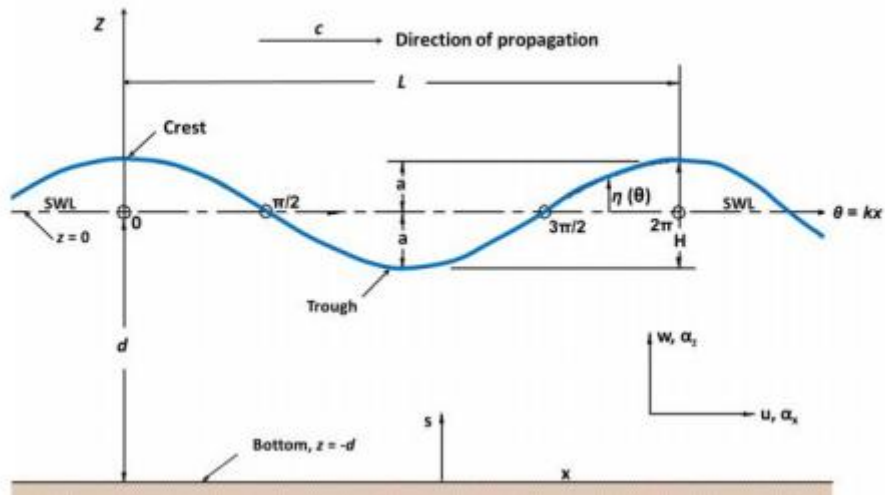


Figure 11: Wave parameters that are fundamental

A sinusoidal wave's surface height as a function of time  $t$  and horizontal distance  $x$  can be expressed (Joubert, 2013a) as follows:

$$\eta = \frac{H}{2} \cos\left(\frac{2\pi x}{L} - \frac{2\pi t}{T}\right) = \frac{H}{2} \cos(kx - \omega t) \quad (10)$$

The horizontal-,  $u$ , and vertical-,  $w$ , components of the fluid velocity can be calculated using the surface elevation and velocity potential equation:

$$u = \frac{H}{2} \frac{gk}{\omega} \frac{\cos hk(d+z)}{\cosh kd} \cos(kx - \omega t) \quad (11)$$

$$w = \frac{H}{2} \frac{gk}{\omega} \frac{\sin(d+z)}{\cosh kd} \sin(kx - \omega t) \quad (12)$$

A regular wave's wavelength ( $L$ ) in any water depth is defined as:

$$L = \frac{gT^2}{2\pi} \tanh\left(\frac{2\pi d}{L}\right) \quad (13)$$

The wave celerity or phase velocity is the speed at which an individual regular wave propagates, as described by:

$$C = \frac{L}{T} = \frac{gT}{2\pi} \tanh(2\pi d/L) \quad (14)$$



### 3.3. Ocean energy generating poses environmental challenges.

In 2009, the US Department of Energy did a study that found that the electromagnetic fields around power-generating equipment and cables that run through the water are dangerous to aquatic life(Ringwood, 2010)(Apunda and Nyangoye, 2018). Electric current flowing via wires generates an ambient magnetic field, which in turn induces a localized electric field in swimming marine life. Eels and sturgeon, for example, have evolved to be very sensitive to electromagnetic fields, so they can't live in any environment that has them(Booij, Ris and Holthuijsen, 1999). Sea turtles use magnetic information to find their way, so if the magnetic field in their natural environment changes, they may get lost. This is especially likely to happen near cables or other structures that create electromagnetic fields.

The toxic effects of technology: Boehlert et al. (2008) state that hydraulic coatings on fish and other aquatic species may result from inadvertent leaks in the turbines' hydraulic systems. When huge marine animals crash into turbine blades, hydraulic fluid may spill into the water and even plug the fish gills, causing them to drown. Biofouling on marine technology equipment and cables is a major environmental issue that physically and chemically depletes the technology, lowering its efficiency. Metal components rust when exposed to biofouling, moving water, and sand particles. To combat the issues of biofouling and corrosion on metallic components, Lewis et al. (2011) and Sundberg et al. (2005) recommend doing thorough research on a material that does not rust in water and has anti-fouling material properties(Apunda and Nyangoye, 2018). The positions of the turbines should be clearly marked on the water's surface, and the maritime authorities responsible for ocean traffic should be made aware of them to reduce the risk of boat and ship accidents. This, as Pelf and Fujita point out, may reduce the risk of ammonia and hydraulic system leakage in the event of a collision between ships (2002).

Alterations to the water's flow and swells: Bryden et al. (2004) state that the networking of technology, which requires many cables and buildings buried under the ocean, disrupts the natural movement of water. Some parts of the permanent structures slow the water down, which is bad for the aquatic habitat. The slowing of ocean currents has negative consequences for both the accumulation of sediments on the ocean floor and the survival of animals that rely on the sea floor for survival. When wave energy goes down, long coast currents shift,

which decreases energy and makes the surface zone bigger. Both of these things change the beach and cause erosion(Apunda and Nyangoye, 2018).

Benthic organisms: Almost all aquatic plants and animals are displaced during the mounting of the structures, the laying of the cables, and the construction of the foundation. Additionally, water circulation is altered by the massive structures, which may be detrimental to bottom-dwelling species and lead to an increase in sediment deposition. During operation, the turbines may produce noise that might be disturbing, killing or dispersing most benthic creatures in the region. Because of the huge structures, water currents around the static structures will be turbulent, washing away even more benthic species.

The sounds they make are their only means of communication among members of their own species. The ability to hear is crucial to their development, safety, movement, feeding, and communication. The noise from ocean turbines gets in the way of these things and, in the worst cases, can be harmful.

An increase in sea temperatures The created warm water will naturally mix with the cold water and rise to the top, forcing the cold water from the surface to sink to the bottom, in a process known as ocean thermal energy conversion on a massive scale. Long periods of mixing may raise the temperature of the water at the bottom, which can cool the water at the top. They can only undertake their research in still water(Apunda and Nyangoye, 2018). A further detrimental effect of high temperatures on reproduction is that they may hinder eggs from hatching and larvae from maturing. But most aquatic species breed in places where humans don't mess with them much, where there are lots of aquatic plants, and where the speed of the ocean current is slower than what is expected in the turbine area(Apunda and Nyangoye, 2018).

### 3.4. Aspects of economics

The cost of tidal energy devices is heavily influenced by these factors: The size of the reserve and how consistent it is. Maintenance and manufacture of tidal to electrical energy converters. Transmission of power from the point of generation to the general population.

A number of places throughout the world, for example, do not have enough ocean energy to support cost-effective tidal generating equipment. While the tides are fairly predictable, relying on the energy collected by wave-triggered instruments can be disastrous, especially when the ocean is completely calm and quiet.

Other energy sources, such as solar and wind energy, may also face this problem. Furthermore, the calm oceans are considerably more likely to see an unwanted incident than the winds on a gloomy day. However, the option exists, and investing in standby classification may be necessary.

The most essential aspect in producing wave energy is capital expenditure. There is a clear difference between fossil fuel methods, where the cost of the fuel is the primary factor. However, due to study and modifications to existing models, it is now more cost effective than previous versions. The majority of the money will be spent on the device's construction, installation, and connection to the electrical grid; the gadget must be long-lasting, flexible, and weather-resistant. There are further costs linked with the plant's location.

Also, because seawater is corrosive, there is a demand for maintenance: rust forms on the device's surface; the power of waves. Maintenance includes removing any aquatic animals that may have gotten stuck on the devices and limiting the generation of sea luminary. The marine machinery, on the other hand, is modern, well-built, and long-lasting. One must consider ships, vessels, docks, and oilrigs that have been in service for several years and require just minimal maintenance to keep them operational. In the case of oil extraction areas, in particular, it is likely that energy sector organizations who have overseen maintenance and development will be able to increase their understanding of this reusable reserve.

It would be more cost effective to form cooperative ventures between tidal plants and offshore devices. It might be possible, for example, to fit the turbines under offshore wind farms. Because the windiest regions tend to have the largest waves, this will provide the best conditions for the two technologies to work. The tides fences can also be used as bridges.

### 3.5. Conclusion

The purpose of this section is to provide a snapshot of the available information on ocean currents and wave energy along the South African coast. This analysis will focus on the Agulhas Current since previous research has indicated that the typical flow rates of the Benguela Current are insufficient to power marine turbines (Meyer *et al.*, 2013). Since the Benguela Current's typical speeds range from 0.11 to 0.23 m/s and its transports from 15 to 20 Sv, it is not strong enough to power naval turbines and will not be explored further. The

Agulhas Current has a transfer value of about 70 SV, making it stronger than the Benguela Current.

In particular, South Africa's major ports needed access to real-time wave and wind data in order to optimize vessel operations. At the request of the Transnet National Ports Authority, the CSIR constructed the Integrated Port Operation Support System (IPOSS) at all of the major ports shown in Figure 6. Several wave stations along the South African coast were placed in strategic locations, such as near harbors and offshore buildings, and are successfully maintained and monitored as part of the CSIR wave recording network, also known as the CSIR Wave Net. This is still the main way that researchers in South Africa get information on waves(Meyer *et al.*, 2013).

Therefore, it is evident that the emergence of ocean energy generation has posed serious environmental challenges to aquatic life, including the induction of an electromagnetic field in the ocean water due to current flowing through the cables; the interference with water currents and waves from new technological structures submerged in the ocean; and the displacement and destruction of the natural habitat of benthic organisms. More research is needed to reduce the environmental impacts observed during commissioning, decommissioning, and operation(Meyer *et al.*, 2013).

## 4. Chapter Four: Analysis of measured wave and current data

The CSIR's five wave monitoring stations run on behalf of Portnet were used to estimate South Africa's most energetic coastline zone in this study. These stations' wave data were judged typical of the country's numerous coastal areas, which include the west, southwest, south, and east coastlines. The relative placements of the stations are depicted in Figure 12.

Table 2: Information about wave recording stations that is relevant

Recording station	Lat Long coordinates	Distance offshore (km)	Water depth (m)	Description of data	Recording period	% coverage	Wave recorder
Port Nolloth	29° 46.8'S 16° 46'E	30	100	3 Hourly $H_{m0}$ and $T_p$	1987/04/08 to 1996/08/31	63%	Waverider
Slangkop	34° 7.6'S 18° 10.6'E	13	170	6 Hourly $H_{m0}$ and $T_p$	1978/10/03 to 1993/06/12	72%	Waverider
Cape point	34° 12.2'S 18° 17.2'E	7	70	3 Hourly $H_{m0}$ and $T_p$	2000/07/01 to 2006/06/30	92%	Waverider
FA platform	34° 58.2'S 22° 10.2'E	72.5	113	1 Hourly $H_{m0}$ , $T_z$ and $H_{max}$	1998/01/01 to 2003/12/31	97%	Radar
Durban	29° 59.2'S 30° 59.9'E	2.3	42	3 Hourly $H_{m0}$ and $T_p$	1992/08/11 to 2001/10/31	69%	Waverider

Bathymetry, or water depth, has a considerable influence on the resultant nearshore wave environment as waves travel from deep sea to shore. As a result, the location of the wave recording stations in respect to the continental shelf has an impact on their exposure. Figure 12 depicts the continental shelf as a light blue region with its margin at about the 200 m depth contour, as seen in Figure 12. The shelf at the Slangkop, Cape Point, and Durban wave recording stations is rather small in compared to the broader area of the Port Nolloth and FA platform recording stations (Meyer *et al.*, 2013).

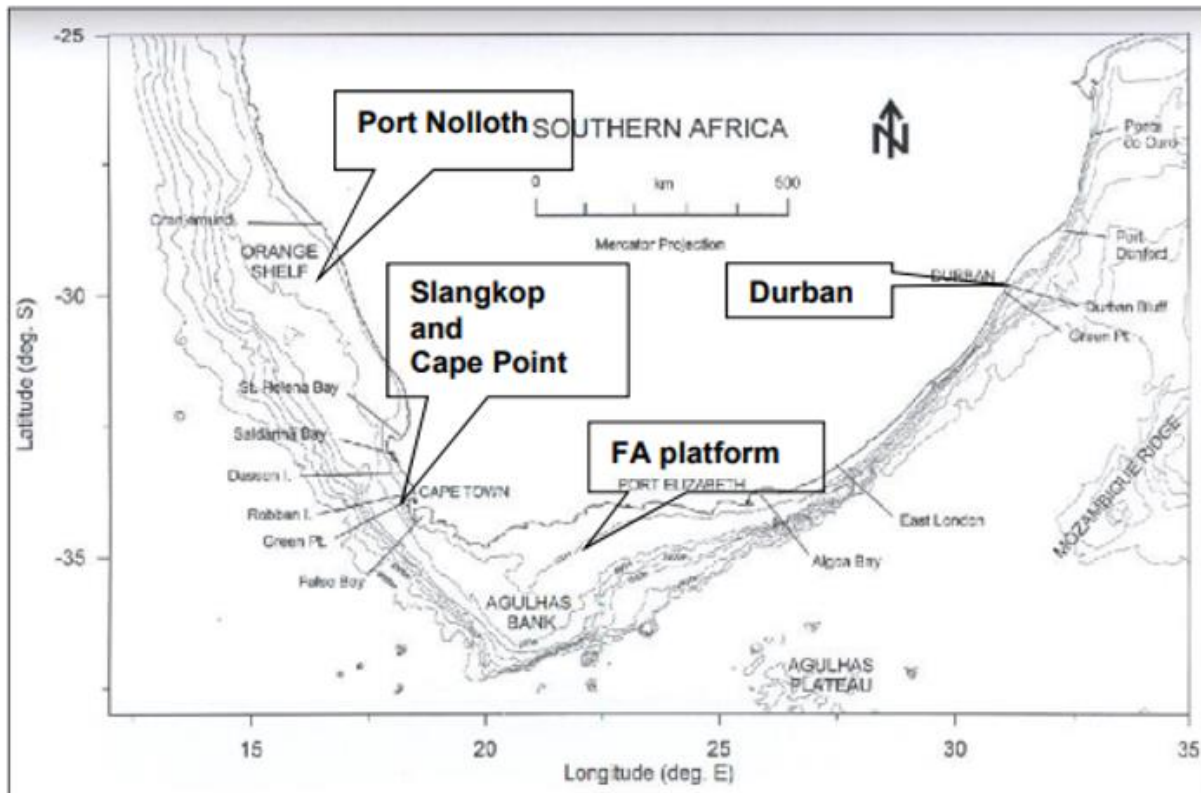


Figure 12: Southern African seabed contours to a depth of 3000 m

#### 4.1. Port Nolloth

The measurements demonstrate the wave energy associated with the west coast of South Africa. Low pressure systems (extratropical cyclones) between 40° and 60° latitude cause waves to move toward the South African coast from the Southern Ocean. These waves are south-westerly (de Vos, Vichi and Rautenbach, 2021). The weather in South Africa is discussed in Chapter 2. 2. As waves move north from the storm's source, they are expected to lose height and, therefore, intensity (Meyer *et al.*, 2013).

#### 4.2. Slangkop

From 1978 through 1993, a buoy known as the Slangkop Wave Rider was stationed about 13 kilometers west of Kommetjie. (Check out Image 13) The Slangkop lighthouse picked up the radio transmission from this buoy. In 1994, the wave recording station at Slangkop was moved to its current location at Cape Point. Slangkop and Cape Point, the two most south-westerly stations, are the first to receive wave power from the prevailing south-westerly direction. Even though the Slangkop recording station was only 13 kilometers from shore, it measured a depth of 170 meters, which shows a sharp drop in height along the continental shelf (see Figure 12) (Meyer *et al.*, 2013).

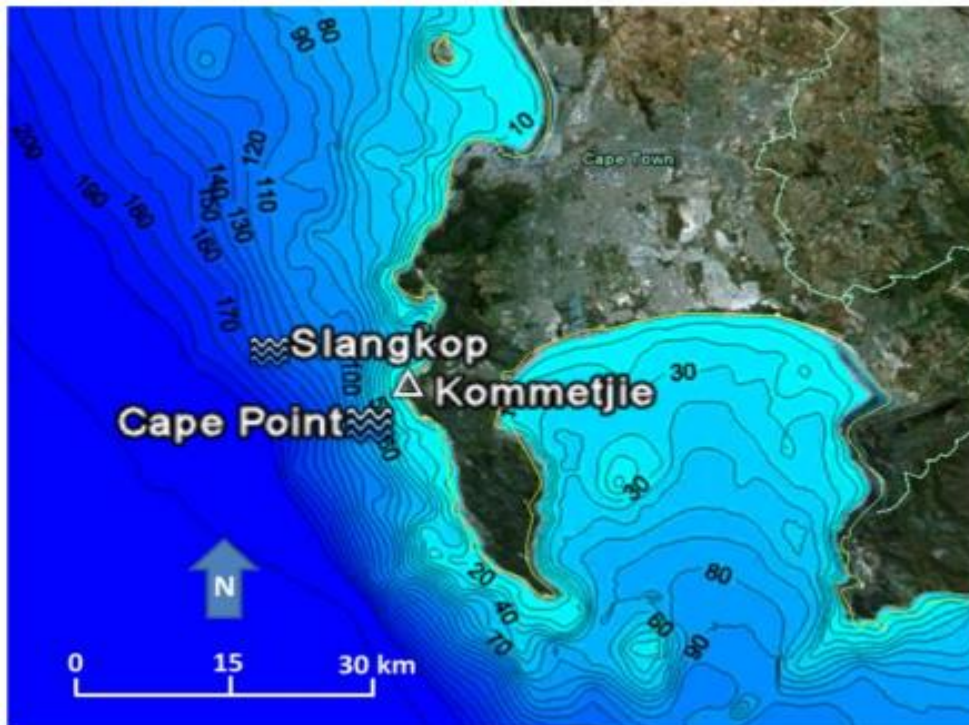


Figure 13: Slangkop and Cape Point wave recording stations' locations

#### 4.3. Cape Point

The Cape Point recording station's wave rider buoy may be found 7 kilometres southwest of Kommetjie, at a depth of 70 meters. Due to greater losses caused by bottom friction, the Cape Point recording station is expected to be subjected to lower wave power levels than the Slangkop station. On the other hand, the Cape Point station may be more vulnerable to the effects of waves than Slangkop due to the concentration of wave strength by local bathymetric features under certain wave conditions (Meyer *et al.*, 2013). Although it is impossible to directly compare the data from these two stations because of the discrepancy in their recording times, it is reasonable to assume that, due to their proximity, they would be subject to very comparable wave power circumstances (Meyer *et al.*, 2013).

#### 4.4. FA platform

A depth of 113 meters separates the FA platform from land by around 73 kilometres. The platform is used to produce natural gas from substrata beneath the seafloor. A submarine pipeline transports the natural gas to a refinery on land that PetroSA runs at Mossel Ba.

#### 4.5. Durban

The wave climate recorded at the Durban wave recording station indicates the predicted wave power along the beaches of eastern and southern South Africa. Durban is located in a region where southwesterly waves are weaker than at other monitoring locations.



Nonetheless, the destructive potential of tropical storm-generated waves on the Eastern Seaboard must be taken into account. Off the shore of the Durban oil refinery, near to the site of the old Durban Airport, is where you'll find the Waverider buoy at the Durban recording station (i.e. Louis Botha Airport)(Meyer *et al.*, 2013).

#### 4.6. Wave height analysis

Equation 11 shows that the power of a wave is directly proportional to the square of the wave's height(Meyer *et al.*, 2013). An assessment of the wave height distribution at each station along the coast will therefore offer an approximate estimate of the projected wave power conditions at each station(Joubert, 2008). Wave heights are also important design criteria for maximizing wave energy conversion and avoiding destruction. The probability curves for exceeding  $H_{m0}$  at each location are shown in Figure 14. Figure 14 illustrates that the FA platform has the greatest  $H_{m0}$  values and the maximum chance of exceeding, followed by Slangkop, Cape Point, Port Nolloth, and Durban(Niekerk, J. R. Joubert, 2013).

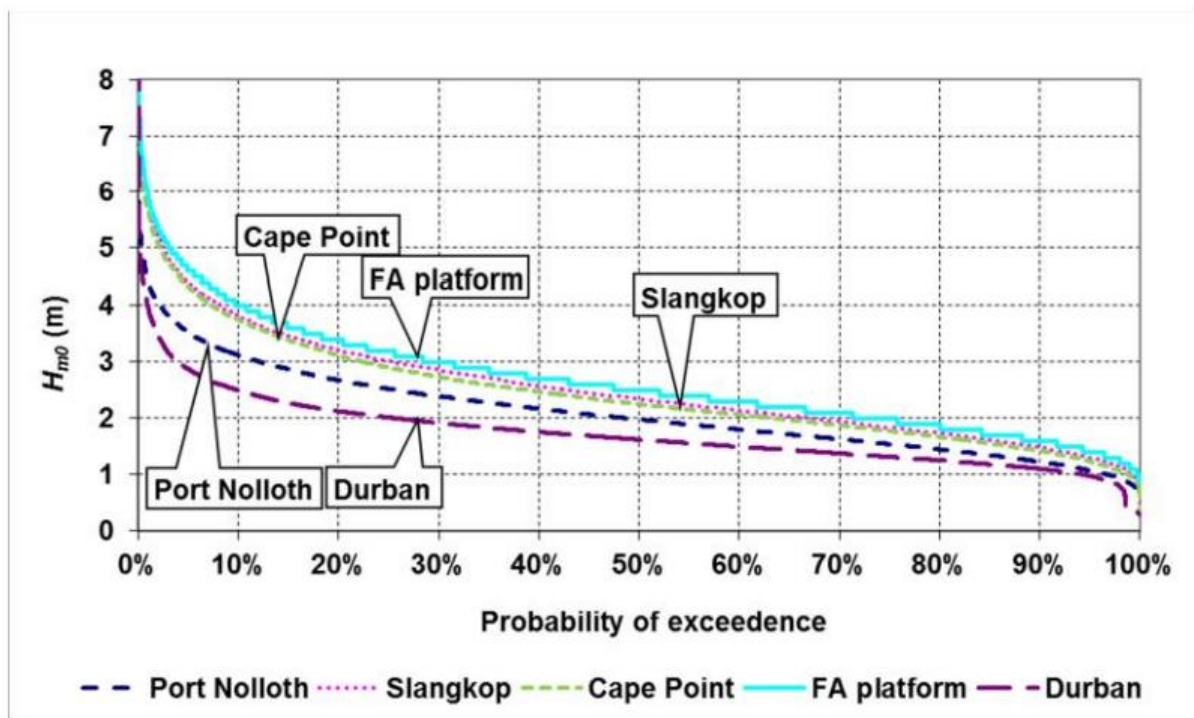


Figure 14: the likelihood that  $H_{m0}$  will be exceeded at each wave recording station

The most frequent wave height at FA Platform, Slangkop, and Cape Point is around 3 m, which happens 40% of the time, as seen in Figure 15. Approximately 2 m is the most frequent  $H_{m0}$  value in Port Nolloth and Durban, occurring 50% and 70% of the time, respectively. On the other hand, the waves are higher in Port Nolloth. Based on this wave height studies, it is



anticipated that the FA platform would have the greatest wave power resource of all the stations.

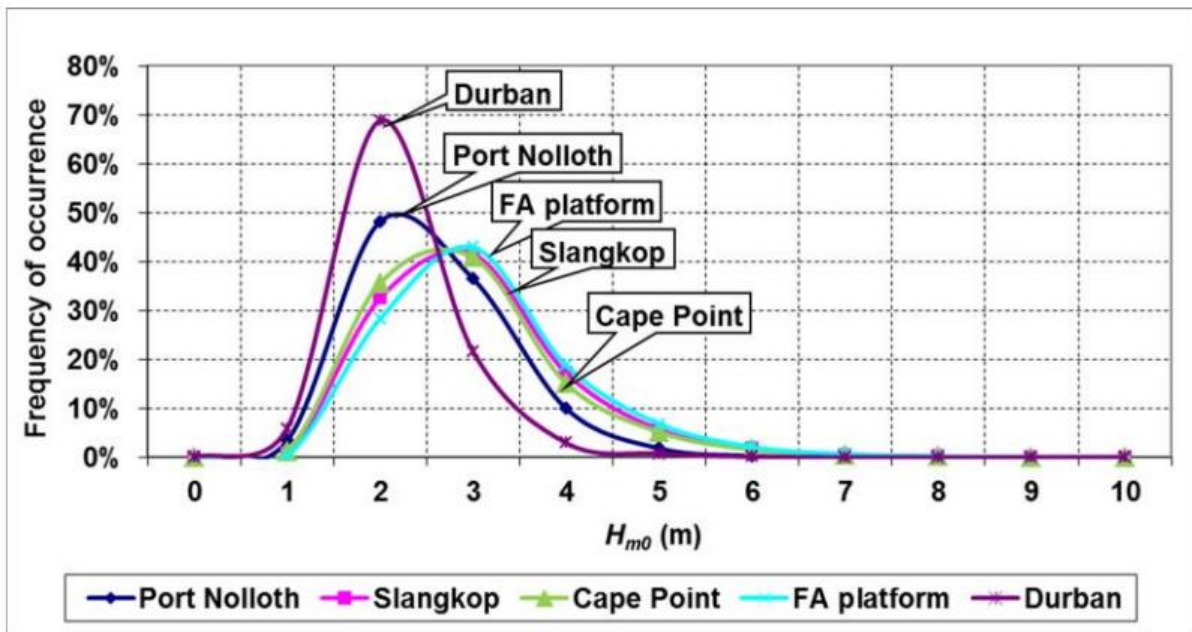


Figure 15:  $H_{m0}$  incidence frequency over all wave recording stations

Since MacHutchon's hundred-year design storm wave height is a crucial design parameter for wave energy devices, Table 3 displays the highest wave heights observed at each station and the matching hundred-year design storm wave height (2006).

Table 3: Measured wave data is used to create wave heights.

Stations	Max $H_{m0}$ recorded (m)	$H_{1/100}$ (m)
FA platform	12.7	11.0
Durban	7.3	7.7
Cape Point	11.0	11.7
Slangkop	10.9	11.9
Port Nolloth	7.4	9.4

#### 4.7. Wave period analysis

This metric can be used to assess the potential of an energy resource. The reaction of wave energy devices is very sensitive to the current wave period. Many devices are designed to achieve a resonant response, which occurs when the system's natural period coincides with the period of the incident wave (Meyer *et al.*, 2013). Device performance is enhanced by

tuning the response to the dominant wave periods. The length of the waves that hit the object is an important design factor. This length is determined by the wave period (de Vos, Vichi and Rautenbach, 2021).

It can be seen in Figure 16 that the peak wave duration is approximately 12 s in Port Nolloth, Slangkop, and Cape Point, but only around 9 s at the FA platform stations farther to the east and in Durban. Dispersion of wave power should be reduced due to the platform's lower  $T_p$  value compared to the recording stations at Slangkop and Cape Point. At Port Nolloth, Slangkop, Cape Point, the FA platform, and Durban's typical wavelengths were 223, 225, 217, 126, and 123 meters, respectively, depending on wave period and water depth (Fairhurst, 2015).

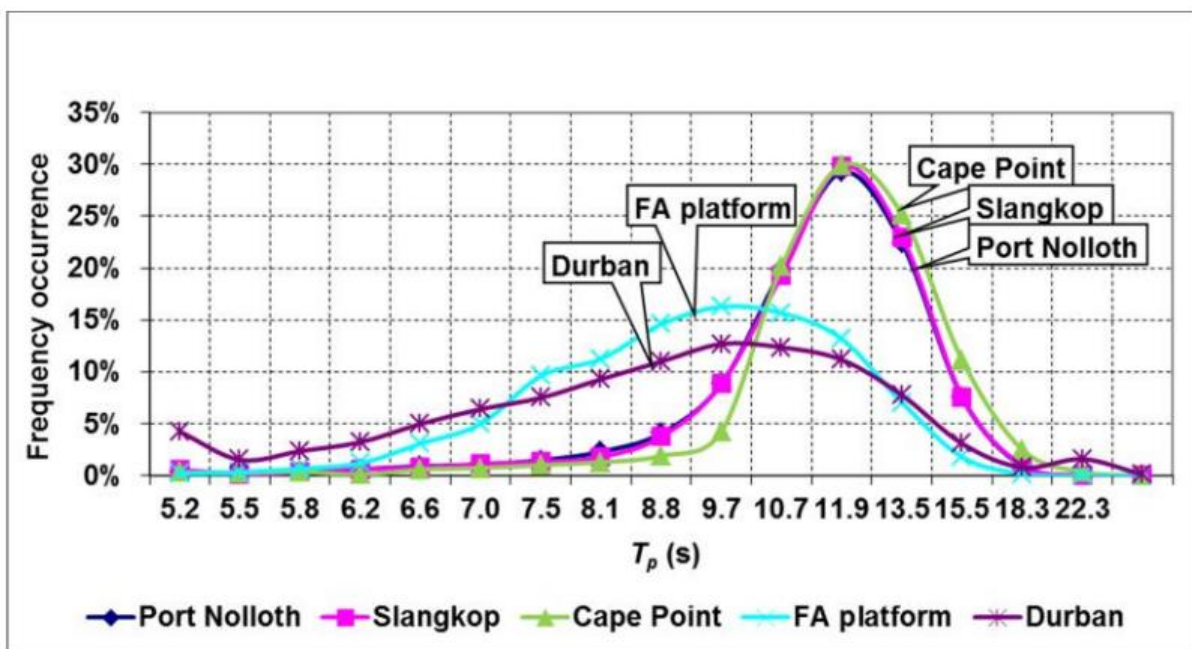


Figure 16:  $T_p$  occurrence frequency at all wave recording stations

Rossouw claims that the measured wave heights and periods off the coast of South Africa agree well with  $T_p$  and  $H_{m0}$  (2015). Analyzing wave power as a function of several aspects of wave periods ( $T_p$ ,  $T_e$ , and  $T_m$ ) reveals the sensitivity of wave power to these properties. Calculations of wave power at the Slangkop recording station for three different wave heights using Equation 11 are shown in Table 4. When it comes to wave strength,  $T_p$  is king, whereas  $T_e$  and  $T_m$  are more cautious. When compared to  $T_m$ ,  $T_e$  generates 20% greater wave power (Meyer *et al.*, 2013). Two writers that argue for using  $T_e$  in wave power estimations are Payne (2008) and Pitt (2017), (2019).

Table 4: The strength of the wave as a function of  $T_p$ ,  $T_e$ , and  $T_m$

$H_{m0}(m)$	$P(kW/m)T_p = 12s$	$P(kW/m)T_e = 10.44s$	$P(kW/m)T_m = 8.4s$
3	22.67	21.02	17.33
5	93.56	80.45	64.78
7	215,32	186.23	156.12

All of the variables that can be manipulated to change the wave's power have been considered. In the next part, we will compare the wave power distribution across the different stations.

#### 4.8. Wave power analysis

The Port Nolloth recording station benefits from a favorable wave power distribution, with a dominating  $T_p$  value of 12s. The wave height and power analysis demonstrated that the Port Nolloth recording station is subject to an energetic wave regime, despite the fact that the wave power decreases with increasing distance from the storm development zone in the southern seas (Joubert, 2008). Wave height and energy analysis show that Slangkop station is often hit by powerful waves. Therefore, it seems that Slangkop station possesses a viable wave power resource for producing energy. In order to survive, however, WEC units deployed in the region would need the ability to detune under excessive stress (Joubert, 2008). Due to how close Cape Point and Slangkop are to each other, we can find strong similarities between the times, heights, and power distributions of waves recorded at Cape Point and Slangkop (Joubert, 2008). Although Slangkop and Cape Point have somewhat different wave power distributions, there is no overlap in the recording periods to allow for a direct comparison of the data.

#### 4.9. Conclusion

The following conclusions may be taken from the analysis's findings, as described in the preceding section:

- Two southwesterly wave recording stations, Cape Point and Slangkop, have the most wave power because they are close to the storm-making area in the Southern Atlantic Ocean.
- The FA Platform has somewhat less powerful waves than Cape Point and Slangkop.

- The WEDI research found that Port Nolloth would be the wave recording station that would produce the greatest electricity from waves despite its poor storm wave energy flow and relatively low average wave power.
- The east coast and the Durban recording station have a very small wave power resource, with an average wave power of roughly 14 kW/m.

The fact that the South West Coast of Africa was chosen as the place with the most potential for using wave power shows that the study did what it set out to do.

## 5. Chapter Five: The spatial distribution of wave power off South Africa's most active coastal zone

An overview of the wave power conditions at places with accessible wave data is presented in Chapter 4 based on the results of the measured wave data analysis. According to the results, the Southwest coast has the greatest potential for wave power. Wave data from the Slangkop and Cape Point recording stations may give us a rough idea of the expected wave power exposure for the southwest coastal area. In order to find the best spots for converting wave energy, it is necessary to do a detailed analysis of the spatial wave power distribution throughout the whole area (Meyer *et al.*, 2013).

This is achieved by the use of numerical modelling of ocean wave propagation along the aforementioned coastline. For the numerical model to accurately reproduce the propagation of waves from deep water (offshore) to shallow water (near-shore), data from the ocean's oceans must be supplied. The depth at which the deep sea wave data is entered must be one at which wave-bottom interaction is negligible. It is not believed that the wave data from Slangkop and Cape Point is the most relevant since they are so near to the shore (de Vos, Vichi and Rautenbach, 2021). On the other hand, deep marine areas throughout the globe are represented by global wave models. As a numerical simulation application, this research makes use of hindcast wave data, which is the recorded results of previous global wave models (which are often checked and updated if required) (Joubert, 2008).

The primary focus of the study is an assessment of the wave power resource between Cape Point and Elands Bay. Using data from the past 10 years, the SWAN wave model will be used to simulate how waves move from the deep sea to the shore in the study area. This will allow the wave power environment to be measured (Meyer *et al.*, 2013).

### 5.1. The study relied on data from offshore waves.

Data from the National Centre for Environmental Prediction's offshore wave inputs were used to assess regional wave power distributions (NCEP). The National Climatic and Environmental Prediction (NCEP) office is located under NOAA, the United States government agency responsible for monitoring global climate and environmental conditions. One of NCEP's nine centres, the Environmental Modelling Centre develops, improves, and maintains models of the atmosphere, ocean, and associated systems, as well as data assimilation systems.

Operational ocean wave forecasts are produced by NCEP using the Wave Watch III wave model, which in turn uses operational NCEP products as input. NCEP's Wave Watch III is a next-generation wave model built on top of WAM. The developer of WAVEWATCH III, Tolman (2006), explains the wave model as follows:

" WAVEWATCH III resolves the spectral action density balance equation for wavenumber-direction spectra. This equation makes the implicit assumption that medium characteristics (such as water depth and current) and the wave field itself change on time and spatial scales far larger than that of a single wave variation. One drawback is that the parameterizations of physical processes in the model do not take into account circumstances in which the waves are severely depth-limited. These two key presumptions imply that the model may be applied at spatial scales (grid increments) outside of the surf zone and larger than 1 to 10 km."(National Oceanic and Atmospheric Administration, Marine Modeling and Analysis Branch, 2012).

Since this part of the study focuses on the near-shore resource, extra numerical wave modeling is required to mimic wave propagation from the deep sea NCEP site to the beach. Buoy data, European Remote-Sensing Satellites (ERS2) fast-delivery altimeter (measures height above a defined datum), and scatter meter (measures scatter from the ocean surface) data are used to validate and verify the NCEP global model output. In the next part, we evaluate the NCEP data(Meyer *et al.*, 2013).

#### 5.1.1. Wave data from the National Centre for Environmental Prediction (NCEP) off the coast of the United States

Offshore NCEP wave data in latitudes 340S 17.50E, 330S 17.50E, 320S 17.50E, 310S 17.50E, and 350S 17.50E are fed into the nearshore wave model. Figure 5-1 depicts this scenario. From February 1997 to September 2006, a full decade's worth of data on backward-facing waves was collected. Time, date, major wave height ( $H_{m0}$ ), peak wave period ( $T_p$ ), and major wave direction are all recorded ( $D_p$ ). There are a total of 27,992 recordings in the wave database, representing a completion rate of 100%. NCEP wave characteristics at 340S 17.50E were compared to wave data collected from the Cape Point wave measuring buoy for the time period between July 2000 and July 2006(Joubert, 2013a). The NCEP predicts that the wave heights will be higher than at Cape Point because the waves lose energy as they move to the shallower sea point(Michiorri *et al.*, 2015).



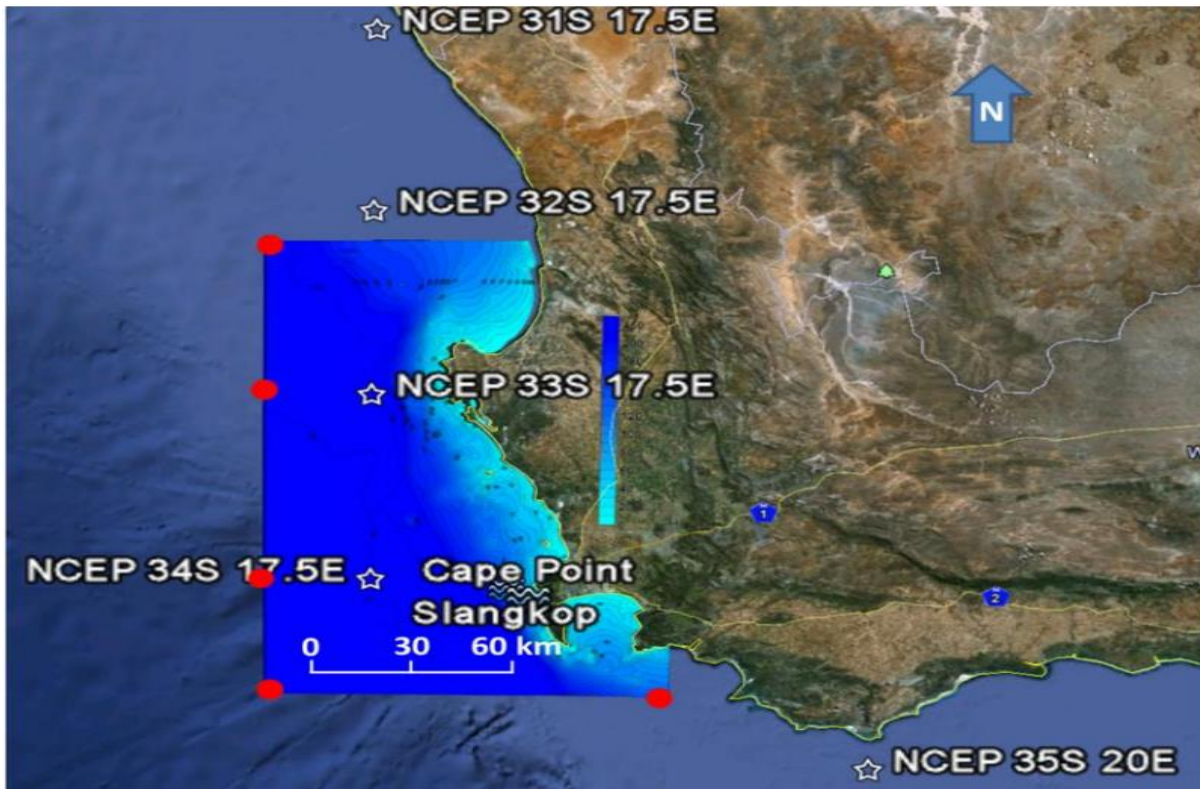


Figure 17: The southwest coastline region, Slangkop, and Cape Point wave recording stations are all indicated by the offshore NCEP data's relative location. On the computational border of the model, red circles denote SWAN input values.

#### 5.1.2. Distribution of wave heights

The height of the waves is a critical factor in determining the availability of resources and in developing appropriate mitigation and adaptation strategies. Therefore, the NCEP wave height data must be of sufficient quality and provide a satisfactory contrast to the wave data recorded at Cape Point (Meyer *et al.*, 2013). As can be seen in Figure 17, the NCEP wave heights are frequently 0.3 m higher than those at Cape Point, as shown by the probability of exceedance curves. As waves approach the shallower seas of Cape Point, their height naturally decreases due to energy losses from bottom friction. When compared to data from Cape Point, NCEP's information on wave height seems to be of good enough quality, with a similar probability of exceeding (Joubert, 2013a).

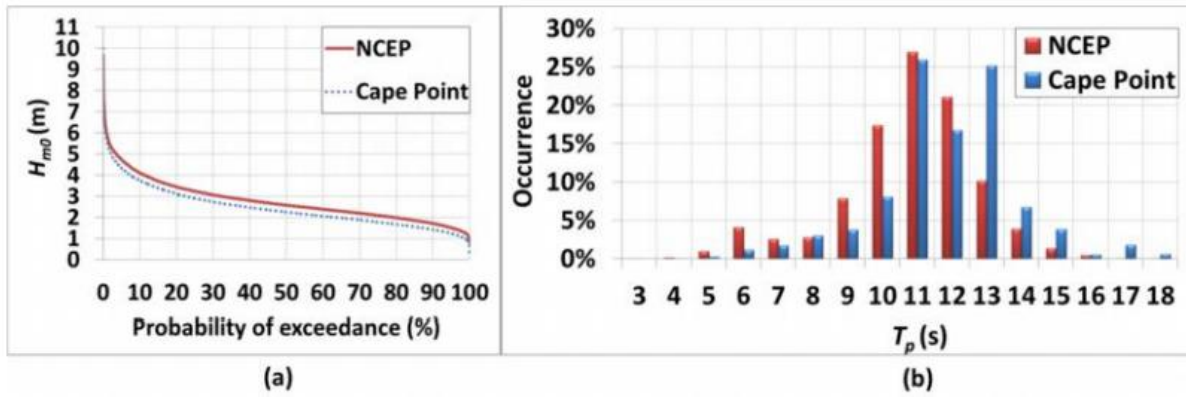


Figure 18:(a) The likelihood that the wave height at NCEP 340S 17.50E will be exceeded as recorded at the wave recording station at Cape Point. (b) Wave period frequency observed at the Cape Point wave recording station from July 2012 to July 2020 at NCEP 34S 17.

According to the NCEP and Cape Point wave period bar graphs displayed in Figure 18, the 11-s period is the most common and occurs around 25% of the time across the six-year timeframe (b). Since Cape Point data often exhibits higher values of wave period, occurring more frequently than NCEP data, it is possible that the NCEP data under-estimates the wave period conditions around the South African coast. This may be because regional effects are not taken into consideration by either the NCEP model or the recording frequency bins for the Cape Point buoy. Most of the time, the NCEP wave period data is better because the frequency distributions of the two sets of data are similar enough (Joubert, 2013b).

### 5.2. The SWAN wave model's history

According to the user handbook for SWAN Cycle III version 40.85, the SWAN (Simulating Waves Nearshore) wave model is used to anticipate wave characteristics in coastal areas, lakes, and estuaries utilizing given wind, bottom, and current variables. SWAN is a system that was created at Delft University of Technology and is always being refined. Unlike most other coastal wave models, SWAN is open-source and offered at no cost to the user. More than 250 schools utilize it for teaching and research, according to scholarly studies. The SWAN model takes into account the nonlinear wave-wave interactions (quadruplets and triads) in the spectral action balance equations, as well as shoaling and refraction (caused by depth and current), wave creation from wind, energy loss from white capping, bottom friction, and wave breaking caused by depth (Joubert, 2013b).

### 5.3. Methodology of wave transfer

The goal of this section of the project was to move NCEP's offshore wave data to the study area so that the geographic distribution of wave strength could be analysed. The simplest way



to do this would be to run a SWAN simulation on all 27,992 of the NCEP data. Such a task would have required too much computing power to be feasible.

The NCEP data on wave directions and periods were binned to reduce the amount of math required (0 s to 30 s in 2 s intervals and 00 to 337.50 in 22.50 intervals). With SWAN and the offshore wave height at NCEP 340S 17.50E, the difference in wave height across the computational grid and at the model boundary was found (de Vos, Vichi and Rautenbach, 2021). For every possible combination of offshore wave period and direction, SWAN outputs the resulting change in wave direction and wave height over the computing zone. The height of the waves in the study area is found by taking a percentage of the offshore input wave height at NCEP 340S 17.50E and expressing it in terms of the variance.

The provided wave modeling technique is based on the premise that offshore wave height variation is directly proportional to a value of one. Energy dissipation mechanisms, such as bottom friction, have a significant role in shaping subsequent wave heights in shallow water and so contribute to the overall wave height. SWAN simulations were run with high-offshore-wave-height inputs to find out how the input offshore wave heights affected the changes in wave height (Treffers, 2009). It was found that the model underestimated the dispersion of bigger waves in shallow water. However, it has been demonstrated that the little changes do not significantly affect the model's overall accuracy.

#### 5.4. Input requirements for SWAN

The creation of a broad description of the anticipated wave power conditions in the study region is the main objective of this research, as was previously indicated. Site-specific designs and real-time simulations were favoured over time-dependent simulations, which were determined to be redundant for this application. Similarly, no wind or current inputs were used in any models (Jak McCarroll *et al.*, 2018). SWAN needs to build a computational domain and corresponding bathymetric grid to forecast wave propagation from input boundary conditions (Joubert, 2013b).

#### 5.5. Validation of the model on the southwest coast

The accuracy of the model was assessed by contrasting its output with information gathered at the Cape Point recording station. As opposed to 70 meters at Cape Point, the model grid point that is closest to the recording station at Cape Point is located 390 meters south of the station at a depth of 78 meters. The NCEP 340S 17.50E data and the Cape Point recording

station's six-year recording period coincide from July 2010 to July 2019. Data gathered throughout this time period will be compared.

The mean monthly median wave power values at Cape Point and the closest model grid point are displayed in Figure 19. When compared to data from Cape Point, Figure 19 shows that the model, on average, overestimates wave strength by 10%.

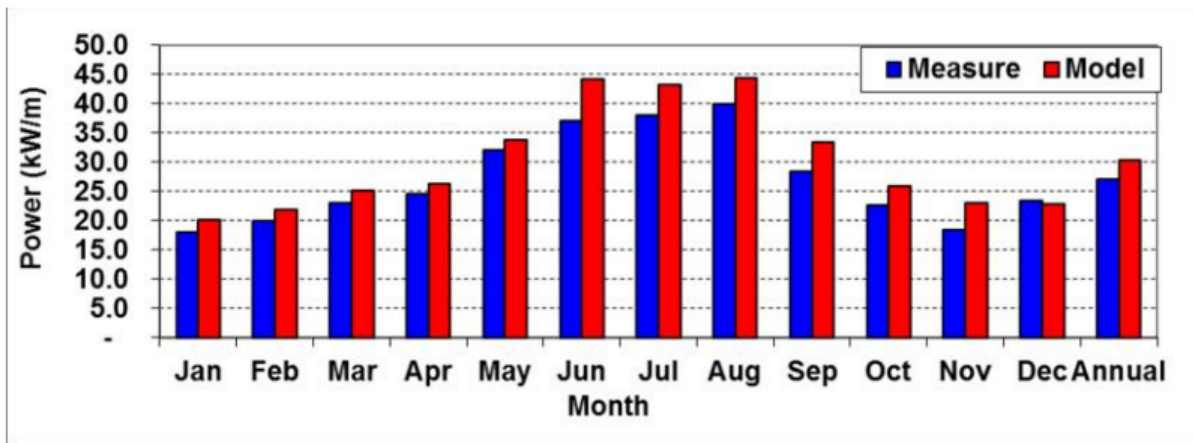


Figure 19: From July 2010 to July 2019, the wave power at Cape Point and the closest model grid point averaged monthly median values.

The wave power at Cape Point was measured and modeled, and the results are shown in Figure 20. Figure 20 shows that the model overestimates the resource for the bulk of data, but it has a high degree of agreement with the real data for low (90%) and high (100% -115%) wave power events (20 percent to 80 percent)(Hsu *et al.*, 2008). In general, the model output met an acceptable level of accuracy for the purposes of this research.

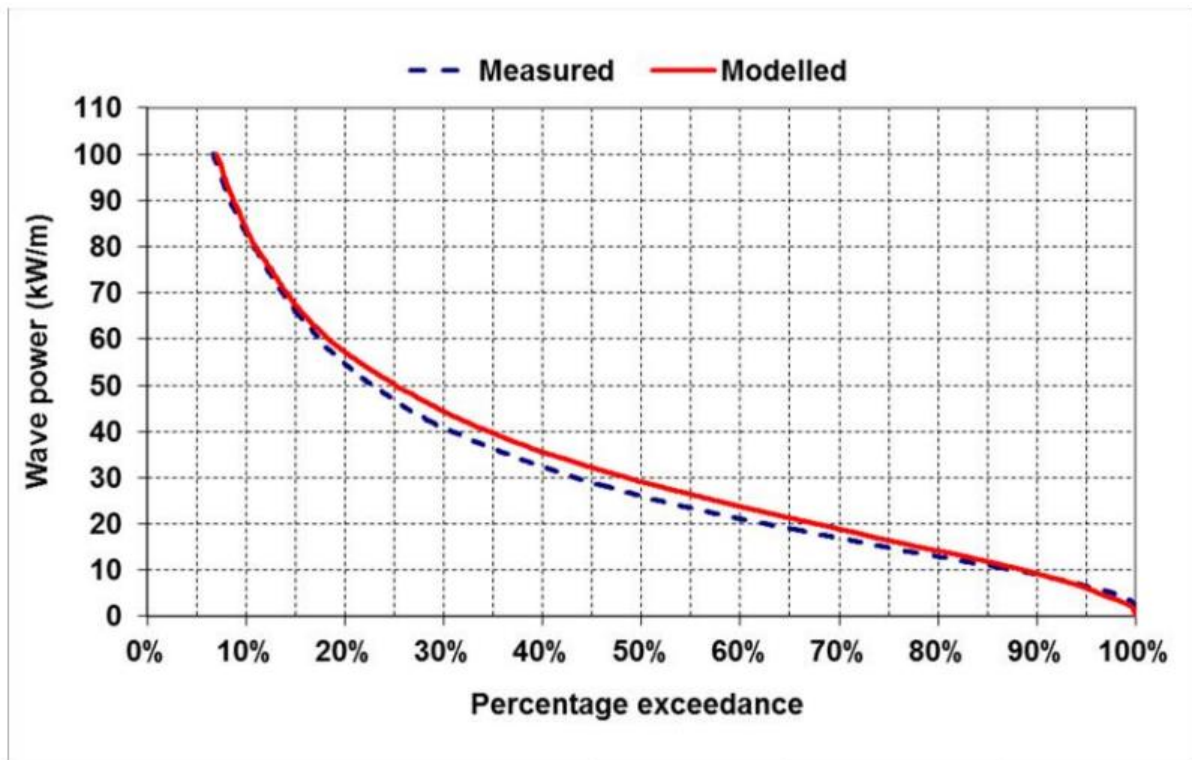


Figure 20: Probability of exceeding wave strength at Cape Point and the closest model grid point from July 2012 to July 2018, as predicted and observed

### 5.6. Conclusion

The precision of the model was evaluated by comparing its predictions to actual data from the Cape Point recording station. The nearest model grid point to the Cape Point recording station is located 390 meters south of the station, at a depth of 78 meters as compared to 70 meters at Cape Point. The NCEP 340S 17.50E data and the recording period at the Cape Point station overlap by six years, from July 2012 to July 2018. The information gathered throughout this time frame will be compared.

Based on Chapter 3's site appraisal, a spectral wave model was created to import 11 years of hindcast NCEP wave data to a specific point in Granger Bay. Wave data was also utilized to estimate the location's wave power potential, which was based on the predicted operational wave circumstances of 0.5 m wave height and an 11 s wave period, with the waves coming in from the northwest. On average, the power of the waves was calculated to be around 2.3 kW/m each year (Joubert, 2013b). The LIMPET site's measured wave power resource of 12 kW/m is far higher. Before figuring out how much power this wave power source could produce, it's important to know how well the device converts the energy.

## 6. Chapter Six: Design

### 6.1. Background of the design

In-depth information on the proposed ShoreSWEC site's ideal wave and water level characteristics is provided in this section. The input pressures, loads, and structural movements were analyzed using Goda's (1974, 1985) equations. Device stability in extreme wave conditions was ensured by carefully selecting the device's size.

#### 6.1.1. Life of design, return period, and likelihood of exceeding expectations

In the ocean, only few wave devices have been in continuous operation. The WEC device that has been in use the longest is the LIMPET, which was set up in 2000. The Carbon Trust (2005) recommended a 25-year design life/operational term (N) for OWCs, which is what the Shore SWEC was projected to have. The stability of the building must be evaluated for a particular design storm with a certain return period (T). The likelihood of this severe event happening during the device's design life must be acceptable. Equation (15) shows that there is a 22 percent chance that the 25-year design life of the Shore SWEC will be exceeded by the one-in-a-hundred (1:100) year storm ('Study of an Electromagnetic Ocean Wave Energy', no date).

$$T = \frac{1}{1 - \sqrt[N]{1 - \frac{P}{100}}} \quad (15)$$

Due to the cost of making sure that structures don't get damaged or fall down, these possibilities and their effects on port development were deemed acceptable.

#### 6.1.2. Hydrographic conditions

The surface height of the shore SWEC is an essential design feature that is heavily influenced by the wave conditions for which the structure is created. Sea level, tide level, and storm surge all have an effect on the total surface elevation used in the design process. Chart datum (CD), the astronomical low tide, is the standard against which all other tide gauges are compared (LAT)(Ogers, 2004).

#### 6.1.3. Water depth

According to the Granger Bay bathymetry shown in Figure 20, the water depth around the breakwater head is 11 m below CD(Joubert, 2013b).

#### 6.1.4. Tidal levels

The South African Navy Hydrographic Office forecasts the following tidal levels for Cape Town in 2018:

Table 5: Tidal levels forecast for Cape Town

Tidal parameter	Level (m CD)
Highest Astronomical Tide (HAT)	2.13
Mean High Water Springs (MHWS)	1.87
Mean High Water Neap (MHWN)	1.33
Mean Level (ML)	0.88
Mean Low Water Neap (MLWN)	0.74
Mean Low Water Spring (MLWS)	0.26
Lowest Astronomical Tide (LAT)	0.1

The structure's crown height and lip submergence depth will be determined in relation to MHWS and MLWS, respectively, to ensure that the most essential water level conditions are taken into account.

#### 6.1.5. Storm surge

According to the CEM, a storm surge is an increase in water level along an exposed shore due to wind stress on the ocean surface. Most of the time, joint probability techniques are used to figure out the relationship between wave height and total water level. For this project, however, it will be assumed that the hundred-year storm surge (SS100) condition will happen at the same time as the hundred-year design wave (Hsu *et al.*, 2008). In order to examine how climate change may affect the city's sea level, the City of Cape Town employed consulting port and coastal engineers Prestedge Retief Dresner Wijnberg (Pty) Ltd (PRDW) (Blake, 2010).

#### 6.1.6. Sea level rise

The ShoreSWEC design must take climate change into account since it affects Cape Town's wave and water levels. The device needs to be built to survive the projected sea level at half its design life, or around 2035, assuming it is developed in 10 years. (Jak McCarroll *et al.*, 2018). According to PRDW's projections, the sea level will increase by 0.27 m by 2035. Offshore wave heights were forecast to grow by 1%, but the storm surge was predicted to fall by 3% due to

weakening local onshore winds. When future sea levels and storm surges are taken into account, the building is expected to be 13.73 meters deep(Blake, 2010).

## 6.2. Offshore design wave conditions

### 6.2.1. Significant wave height

The Shore SWEC system's stability must be assessed in relation to the wave loads assumed during design. SWAN was used to model the propagation of several design storms from offshore to Granger Bay using the computational grids outlined in section 4. This allowed us to identify the most crucial design factors. The directional distribution of severe storm occurrences was analysed by using the maximum wave height that occurred in each directed bin of NCEP data. In Figure 21, it is shown as an ascending wave. Figure 21 shows the wave height that was the highest over a period of 11 years. It was 10.31 m in a west-southwest direction.

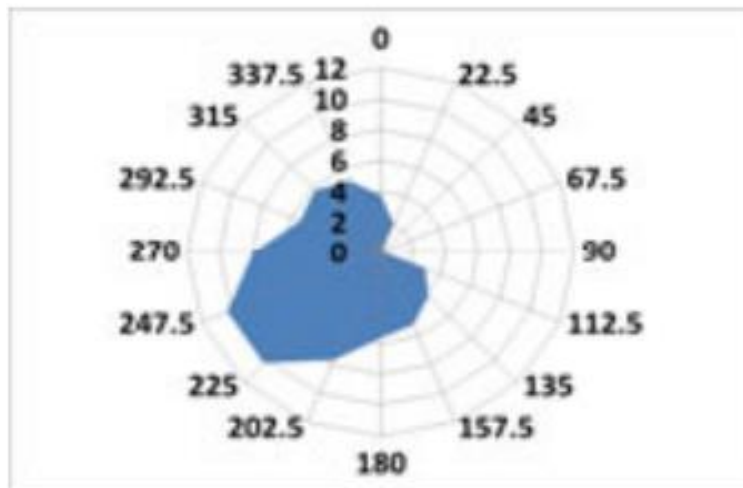


Figure 21: For the 11-year NCEP data, maximum wave height per direction

Since Table Bay faces west, westerly storms are likely to provide the greatest architectural challenges. It has been announced that the infrastructure will be built to withstand a storm that lasts for a century. In his dissertation, Rossouw (1989) suggests that a 100-year wave height of 12 meters offshore is appropriate for South Africa. Because climate change will eventually impact local wind patterns and offshore wave heights, PRDW estimated a 0.1 m increase (2010). The NCEP data revealed that 12.1 m is from west to southwest, hence the hundred-year wave height for each direction was calculated related to this value.

### 6.2.2. Peak wave period

The peak wave period in the design was based on Del Norske Veritas's (2020) highest range of periods:

$$3.6\sqrt{H_{m0}} < T_p < 5.5\sqrt{H_{m0}} \quad (16)$$

$T_p$  and  $H_{m0}$  correspond well with measured wave data off the coast of South Africa, according to Rossouw (1989).

### 6.2.3. Peak enhancement factor

Because of the severe nature of this investigation, it was presumed that the wave energy density spectrum followed the Pierson-Moskowitz (PM) form, suggesting that the wave-field is a true ocean. As a storm progresses, the energy density drops dramatically around the peak frequency.

### 6.2.4. Directional spreading

According to results collected at the Slangkop wave recording station during storm occurrences, the energy density spreading around the peak wave direction ( $D_p$ ) was estimated to be 190 (power m of about 8, see Table B-6).

The results of the SWAN simulations for the 100-year storms from each wave direction are displayed in the next section, along with the associated wave conditions at the Granger Bay location.

## 6.3. Nearshore design wave conditions

According to SWAN output in Table 6, the hundred-year design storm from the west results in the highest wave height at the site, which is 5.32 m. Also, the westerly storm in Granger Bay has a  $T_p$  of 18 seconds, a  $D_p$  of 318.50, and an individual maximum wave height ( $H_{max}$ ) of 8.37 m, which is calculated from 1.8  $H_{m0}$ .

Table 6: circumstances for offshore and nearshore waves in 100 years

	Offshore			Granger Bay	
$D_p(^{\circ})$	$H_{m0}(m)$	$T_p(s)$	$H_{m0}(m)$	$H_{max}(m)$	$D_p(^{\circ})$
0.1	3.89	12	1.04	1.92	303.2
19.45	2.34	9	0.22	0.34	299.88
0.01	0	0.01	0.01	0.00	0.1

68.7	0.01	0.01	0.01	0.00	0.1
89	0.00	0.00	0.00	0.00	0.1
189	7.23	15	0.22	0.08	331.3
201	7.33	14	0.21	0.06	330.2
269	9.32	18	5.32	8.37	318.5
277	6.43	16.5	4.67	7.91	311.5
314	6.44	16.8	4.69	7.96	312.6
321	7.22	17.2	5.4	8.22	316
341.5	5.88	15.4	4.8	6.66	309

The geographical distribution of the  $H_{m0}$  and  $D_p$  produced by SWAN across the computational domains for the westerly hundred-year design storm is shown in Figure 6 on the next page.

The anticipated wave power breakwater's proposed head wave conditions are shown in Table

*Table 7: the Shore SWEC at Granger Bay's design standards*

		Design parameters			
$H_{m0}$	$H_{max}$	$T_p$	$D_p$	$D_{spr}$	Water depth
3.89 m	7.99 m	18 s	129°	13°	14.55 m

Figure 20 shows how waves traveling from the northwest hit the breakwater's head almost perpendicular to the device's longitudinal axis. Given that the 120-degree spread occurs in all directions, the presumed approach angle with respect to a line normal to the structure is 700 degrees. We looked at how these design wave and water level characteristics would affect the wave loads to figure out how well the Shore SWEC could handle an earthquake.

#### 6.4. Design wave loading and dimensional requirements

The most crucial considerations in the design of vertical breakwaters are wave loads and foundation conditions. Massive vertical breakwaters can endure wave stresses because of gravity, friction, and the capability of the rubble foundation to support them. The applied wave pressure, loads, moments, and motions of the structure during intense storms may be



predicted during the early design phase using proven formulas and a quasi-static analysis, assuming a rigid structure. An appropriate factor of safety is maintained by assuming structural dimensions that can support the given loads and testing the structure's stability(Joubert, 2013b).

#### 6.4.1. Type of wave forces

Structure shape and wave conditions interact intricately to determine how much weight waves place on a given structure. In the last stages of design, experimental research in hydraulic labs on unusual structural geometries like the ShoreSWEC is recommended (which is outside the scope of this study). The device design can be modified as a result of having additional knowledge about the wave-structure interaction.

Vertical walls are subjected to three types of stresses: pulsing, impact, and breaking wave. Pulsating or quasi-static strains are produced on structures by nonbreaking waves. Due to its longer length (typically 1/4 or 1/2 of a wave period) than the structure's natural period of oscillation, this may be treated as a static load in stability calculations. Use well-known equations, which will be talked about in more depth later, to figure out the pressure, forces, and moments caused by pulsing loads.

Peak pressures produced by plunging waves that strike a vertical wall are 10 to 100 times higher than those of pulsating waves of the same height because of the extraordinarily high, brief impact loads (0.1 to 1 s) that they create. It is advised to position the structure at an oblique angle of more than 200 degrees to the anticipated wave direction in order to prevent frequent wave breaking on it. The low slope of 1 in 100 at the deployment point will significantly lessen the possibility of waves breaking. The decision tree from Goda and Allsop et al. shows how eliminating breaking waves greatly simplifies the ShoreSWEC stability analysis, requiring just the evaluation of pulsating or broken wave loads.

Because of the depth limitation, offshore breaking waves are subject to much smaller loads than impact or even pulsing loads. This first design process will not account for the broken wave loads. Several ways the device could fail are shown to help the reader understand how important stability is for the ShoreSWEC device(Joubert, 2013b).

#### 6.4.2. Failure modes

Damage resulting in structural performance and functionality below the minimum envisaged by design, and the cost of damage repair, including interference with commercial operation, is unacceptable, and so represents a failure or ultimate limit condition.

#### 6.4.3. Foundation design

The ShoreSWEC was built on a strong foundation that is resistant to toe scour, mounding, and collapse. The CEM (2006c) foundation design method was used. It was presumed that the seabed could support the weight of the structure and any wave-induced transmission stresses due to a lack of geotechnical understanding of the soil properties in Granger Bay. The device will be supported by granular bedding (core layer) that is 15% thicker than the water level at the installation location. This is comparable to the caisson design example in CEM (2006d) and to Takahashi's wave power caisson (1992).

#### 6.4.4. Material

Steel-reinforced concrete will be used in the construction of the ShoreSWEC building. CEM recommends a 65 mm minimum concrete cover in the splash zone to shield the steel reinforcing bars from the corrosive sea spray (2006b). With its high compressive strength (usually 46 MPa after five years) and resistance to sulfates in seawater, ASTM Type V Portland cement will be utilized (CEM, 2006b). Patterson et al. (2009) recommend using low porosity concrete to guarantee concrete longevity and lessen the chance of chloride penetration. To achieve this, a concrete mix with a low water-to-cement ratio is combined with either pulverized fuel ash (PFA) or ground granulated blast furnace slag (GGBFS).

#### 6.4.5. Wall thickness and structural height

Existing OWC structures, OWC breakwaters, and conventional caisson breakwaters, Torre-Enciso et al. (2007), and Takahashi (2002) were used to gauge the device's thickness in contrast to its front and side walls, floor, and crown capping. Additional analysis of these features will be conducted using Finite Element Methods (FEM) during the exact design of the device, which is outside the scope of this investigation. Front and side walls were measured at 0.6 m in thickness, which is considered enough for steel reinforcement and adequate structural strength. The concrete roof and floor were to be twice as thick as the walls (1.2 m), as was the case with similar previous constructions.

The hydraulic reaction of the structure, such as overtopping and wave reflection, is dependent

on its height. Takahashi (1989) recommends a crest elevation (crown height) of  $0.6 H_{\text{design}}$  above the extreme water level for a vertical front wall and  $1 H_{\text{design}}$  for a sloping front wall to maintain an adequate degree of overtopping. Some caisson breakwaters include splash walls, which add height to the structure, to prevent overtopping. The ultimate ShoreSWEC design might include splash barriers and a PTO (consisting of intake and output pipes and a turbo-generator). The impact of these components on the device's steadiness was ignored in this analysis. The effect of these components on the device's steadiness was ignored in this analysis. Takahashi said that ShoreSWEC should have a front wall submergence depth of 25% of the highest wave height expected at the deployment site.

#### 6.4.6. Pulsating wave loads

Initial design work is on determining how much force can be exerted by the ShoreSWEC's ballast chamber under the anticipated wave heights and durations. The difficulty is in creating an affordable large structure that is robust enough to withstand forces brought on by sliding and overturning. 5.4.1 specifies that only nonbreaking, pulsing wave loads should be included in the stability analysis. Goda's (1974, 1985) method of predicting wave forces for nonbreaking waves on vertical barriers is recommended by the British Standard BSI (1991) and the Coastal Engineering Manual (CEM) (2006c). Since Goda's prediction method is the most well-known and generally recognized, it will be utilized to calculate the wave loadings on the ShoreSWEC. The stability study of the ShoreSWEC included two designs with varying dimensions. The front wall of one of them is built in a vertical and sloping fashion. The stability analysis was done using Goda's approach, or a variant thereof. Built-up walls that rise vertically

When waves hit a vertical wall without breaking, the hydrodynamic pressure distribution on that wall is made up of two time-varying parts. hydrostatic pressure, due to the instantaneous depth of the water, and dynamic pressure, due to the accelerations of water particles. Since the front and leeside of a structure below SWL experience equal and opposite hydrostatic pressure, it cancels out, and only the wave-induced hydrodynamic pressure needs to be considered in stability calculations. We can figure out the pressure distribution, forces, and overturning moments caused by erratic waves that don't break on vertical walls by using methods developed by Goda in 1974.

## 7. Chapter Seven: Results and Discussion

### 7.1. Outcomes of the model research

The statistical results of NCEP simulations are primarily used to locate promising coastal locations in the study region for a variety of ocean energy converters (OECs). Incorporating statistical data with the bathymetric contour map, wave farm developers may identify areas with adequate water depth appropriate for their OEC of choice. This research's statistical wave power output may be utilized to determine the wave power resource capacity of a WEC at a given site. It is possible to invert this process by first identifying areas with high wave power; the corresponding water depth then determines the optimal WEC design for these areas. The bathymetry of the major research area is shown in Figure 22.

Similar to the data analysis in Chapter 3, it was decided to only consider three statistical features of wave power: average, 90%, and 5% risk of exceeding. These elements stand in for the minimum allowable power levels, the worst-case scenarios, and the expected average circumstances. Statistics were set up on a monthly and annual basis. Maps showing the average monthly wave power are included.

Some of the results of this study for the area in question are a collection of spatial wave power maps for certain time periods and years that are linked in the thesis (South West Coast). Using data from the previous decade, we were able to determine the following: The mean wave power in the study area was mapped, revealing where it was concentrated and where it had travelled:

- Twelve-monthly average maps (i.e., the average of 10 January months, 10 February months, etc.).
- Annual (10 annual maps using the 10-year hindcast data) (10 annual maps using the 10-year hindcast data) There are 10 yearly maps for the 10-year backcast.
- Average yearly (average over the past ten years of data).

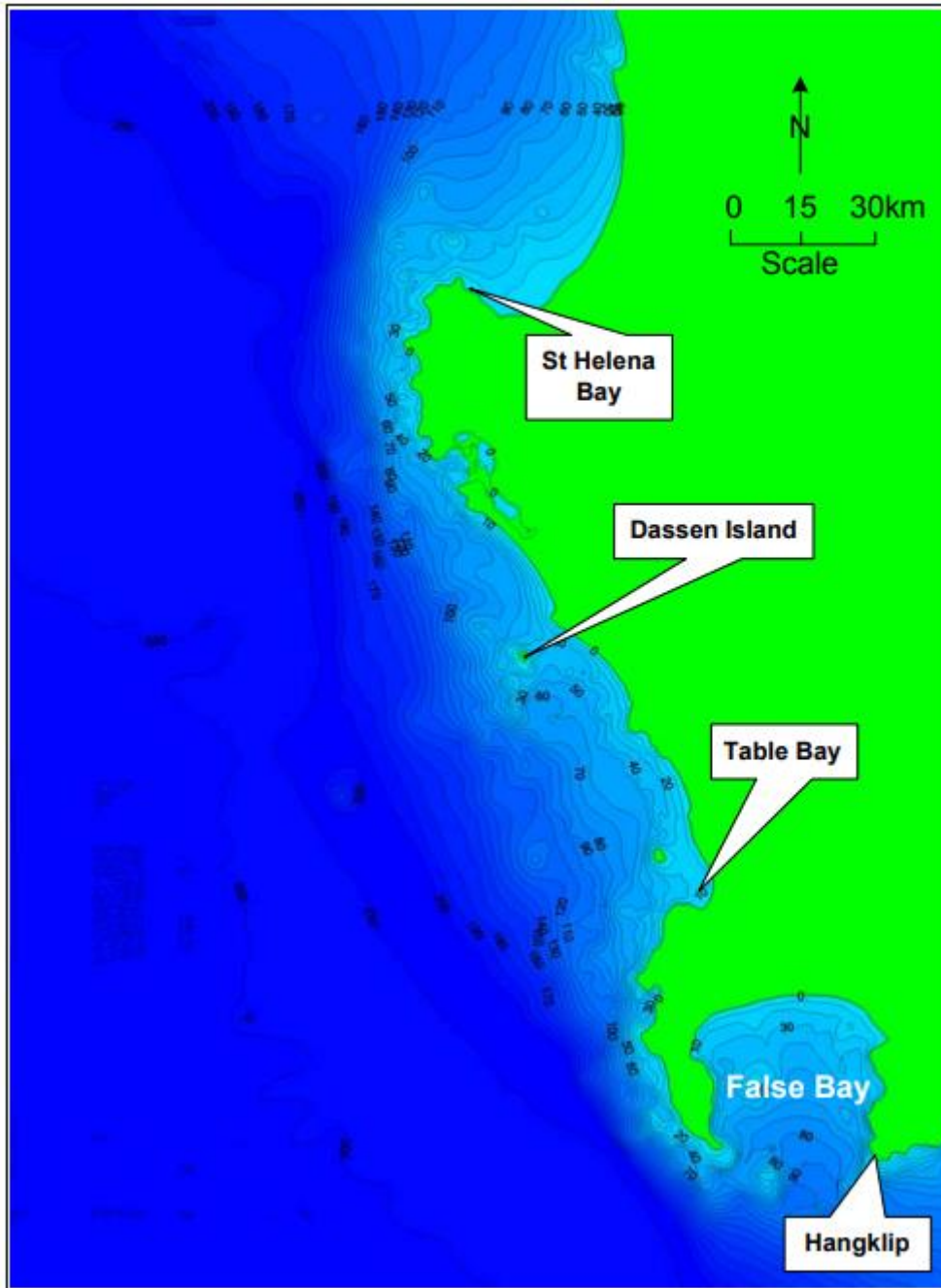


Figure 22:a contour map showing the research area's bathymetry

#### 7.1.1. average wave power per year

The seasonal and geographical pattern of average wave strength throughout the South West Coast over the course of a decade is shown in Figures 23–26. From the contour map of average wave power exposure shown in Figure 23, we can deduce that the deep sea resource is between 20 and 27 kW/m in the summer. Power generation from WEC units should remain stable throughout the year. At such low power levels, the body's own power production is at its peak.

The average wave power distributions of spring and fall are very similar, as shown by Figures 25 and 26. Therefore, if a WEC unit is built for these seasons, it will produce electricity at its best for half the year. In the spring and fall, the deep sea waves resource averages between 31 and 39 kW/m(Joubert, 2008).

The ability of WEC units installed in the research region to survive the winter owing to significant wave power exposure will be put to the test. This is shown in Figure 25 below. Wintertime deep sea wave power resources range from 50 to 61 kW/m. This is twice as much wave strength as in the summer(Joubert, 2008).

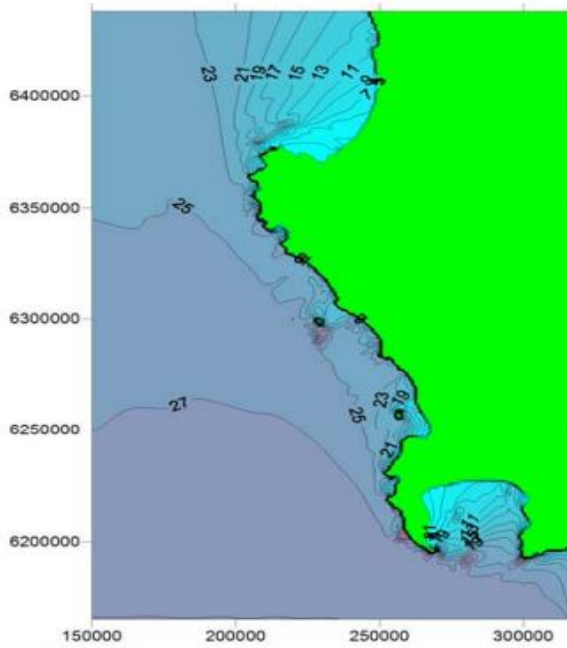


Figure 23: Summertime spatial distribution of the mean seasonal average wave power (kW/m)

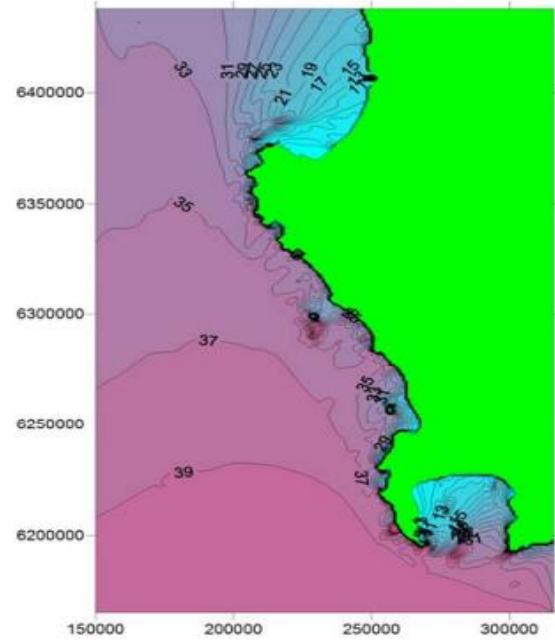


Figure 24: Seasonal average wave power (kW/m) for fall, distributed spatially

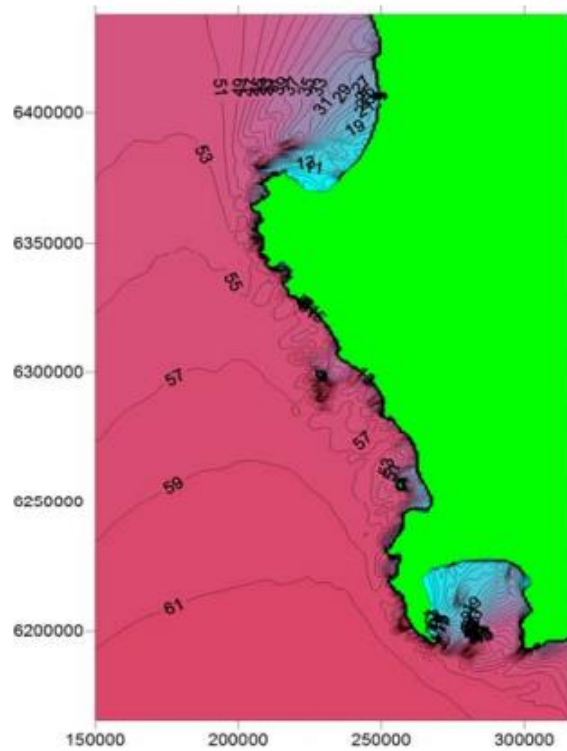


Figure 25: Winter-specific spatial distribution of the mean seasonal average wave power (kW/m)

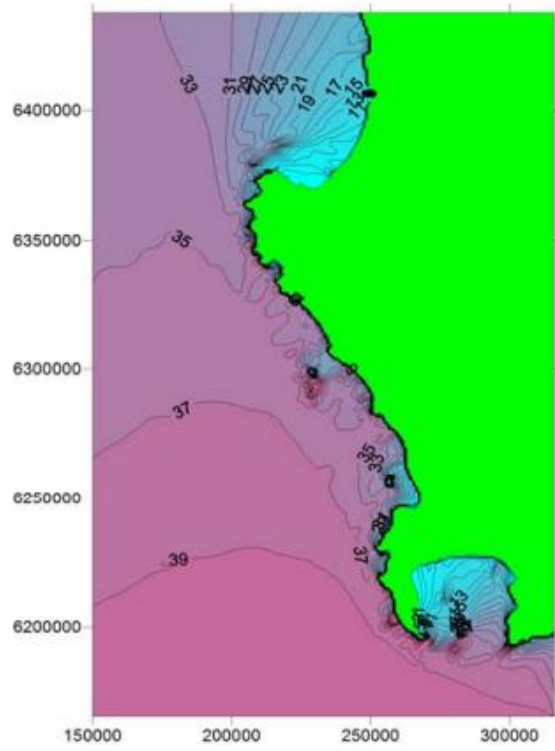


Figure 26: Early summer annual mean energy production (kW/m) spatial dispersion

In 5.1, we examine how well the model hindcast data matches up to the observed data from the Cape Point recording station for the overlapping recording period.

Power at the model grid point closest to the Cape Point recording station is shown in Figure 27 during a 10 year time span. The maximum wave power scenario investigated was 100 kW/m for the reasons given in subsection 3.3. What Figure 27 Shows

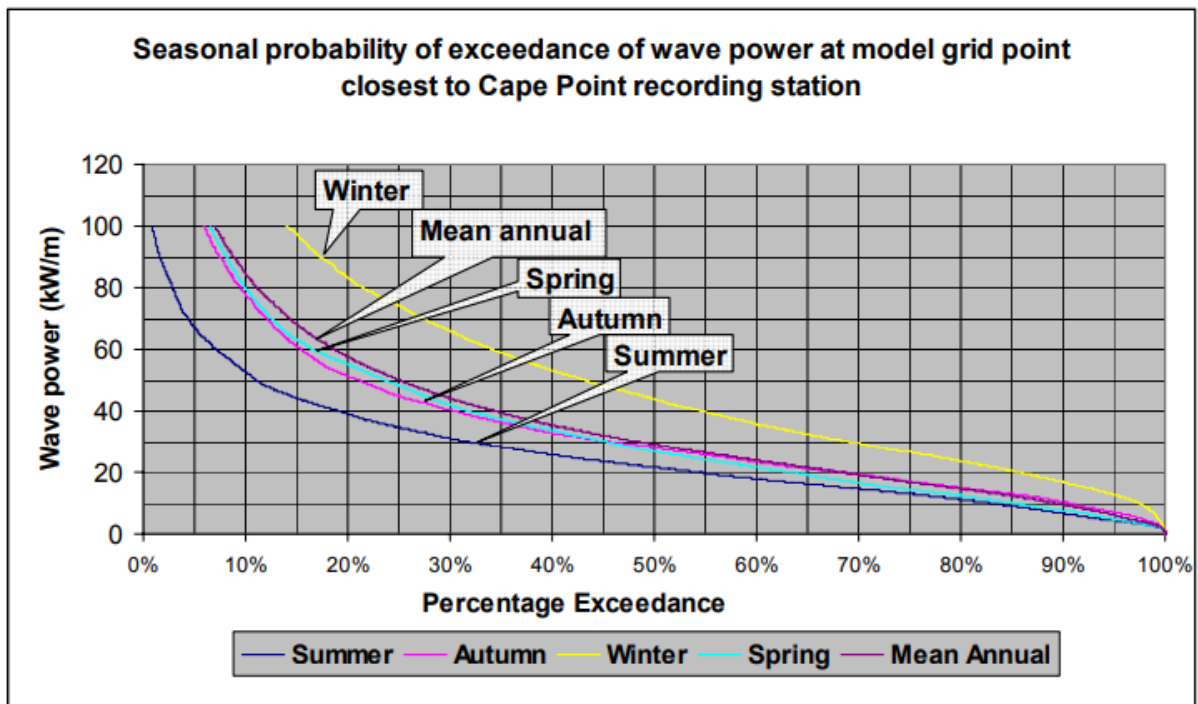


Figure 27: Seasonal likelihood of exceeding wave power at the nearest model grid cell to the Cape Point recording station

The greatest available wave power is in the winter. There is almost a little difference in the annual, autumnal, and springtime probabilities of exceeding curves. In Table 8, we can see that the chances of exceeding the most extreme seasonal wave power events are 6% and 2%, respectively.

Table 8: Extreme seasonal wave power occurrences have a 6% and 2% chance of exceeding the model grid point nearest to the Cape Point recording station, respectively.

Season	2% Exceed	6% Exceed
Summer	96.98	66.5
Autumn	167.88	105.98
Winter	274.44	152.4
Spring	172.33	111.23
Mean annual	193.4	113.57



### 7.1.2. Annual average wave power

From January through April, July and October, we provide the monthly mean geographical distribution of average wave power for the South West coastal area during a 10-year period. These months represent summer, fall, winter, and spring. Notice how the mean seasonal spatial maps are similar to the mean monthly spatial maps. Below, Figure 28 displays the statistics for the mean monthly wave power over a ten-year period at the model grid point closest to the Cape recording station.

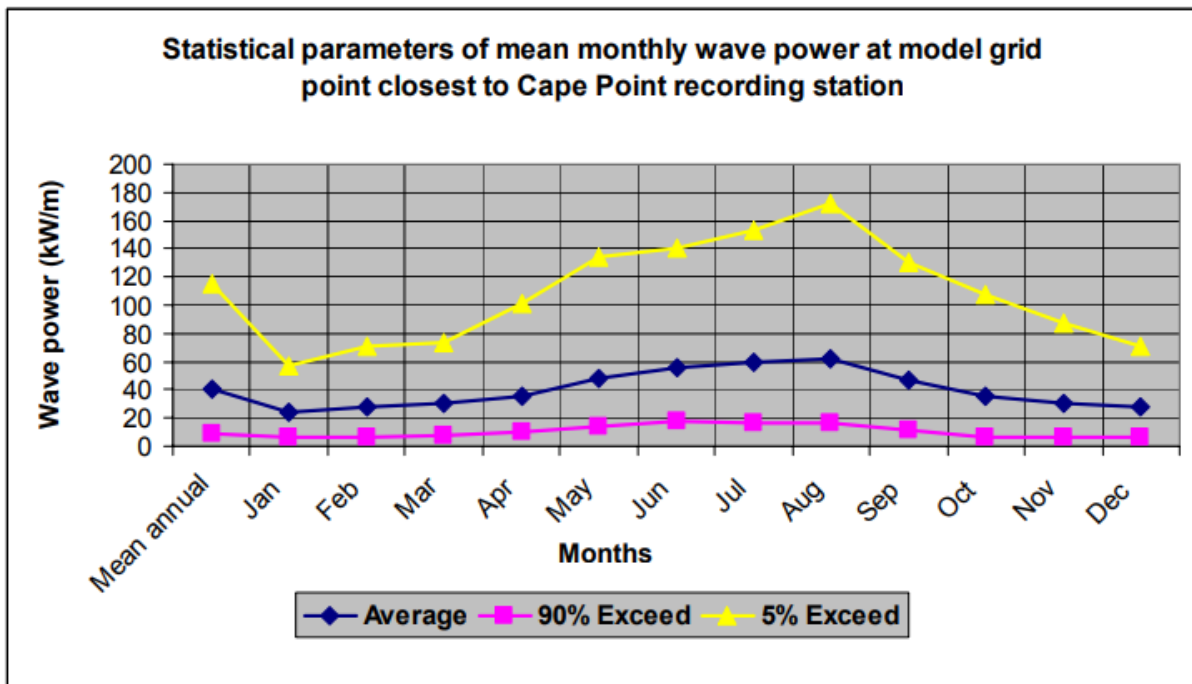


Figure 28: statistical characteristics of the predicted mean monthly wave power

The next step compares the model to real data collected at Cape Point during the same time period. This shows how accurate the model is.

### 7.1.3. Monthly average wave power

As a representative of the fluctuations in wave strength over the course of a typical year, the mean monthly median values for all the stations are shown in Figure 28. According to Figure 29, the winter months of June, July, and August are the busiest, followed by the autumn, spring, and summer seasons. Once again, Slangkop and Cape Point have the greatest mean monthly wave power dispersion.

As shown in Figure 29, the minimum expected mean monthly wave power is stated in terms of a 90% possibility of surpassing it. The average monthly variation in wave power is shown

in Figure 30 by the standard deviation for each location. Slangkop and Cape Point have the largest resources of any areas in the country(Chen *et al.*, 2022). As a result, the wave energy equipment utilized here has to perform reliably across a wide range of wave conditions. Even while Port Nolloth's resources are lower than those of the southwest stations, they are more stable and less prone to fluctuations(Meyer *et al.*, 2013).

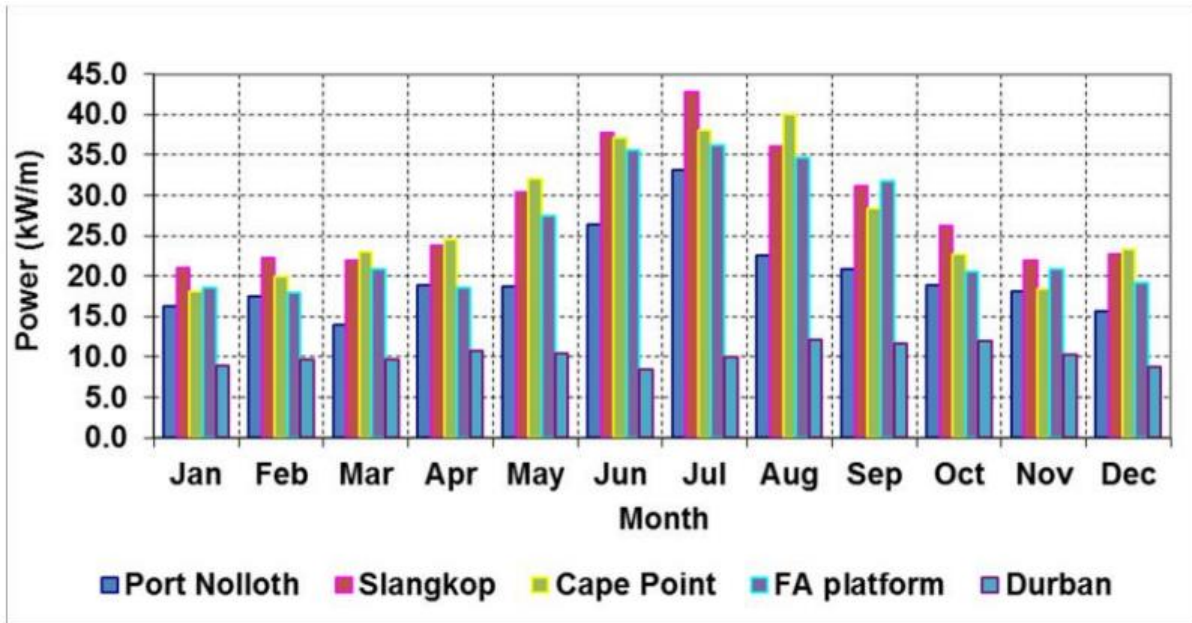


Figure 29: Wave power average monthly averages for the several wave measurement sites

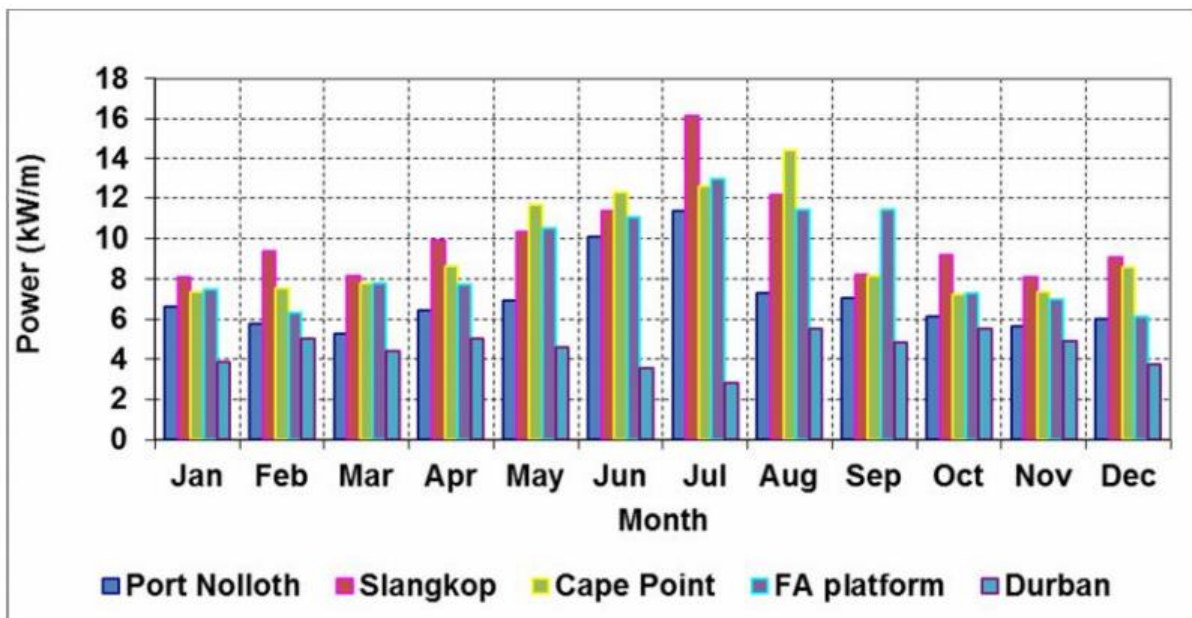


Figure 30: Mean monthly 90% likelihood of wave power exceedance readings for the various stations

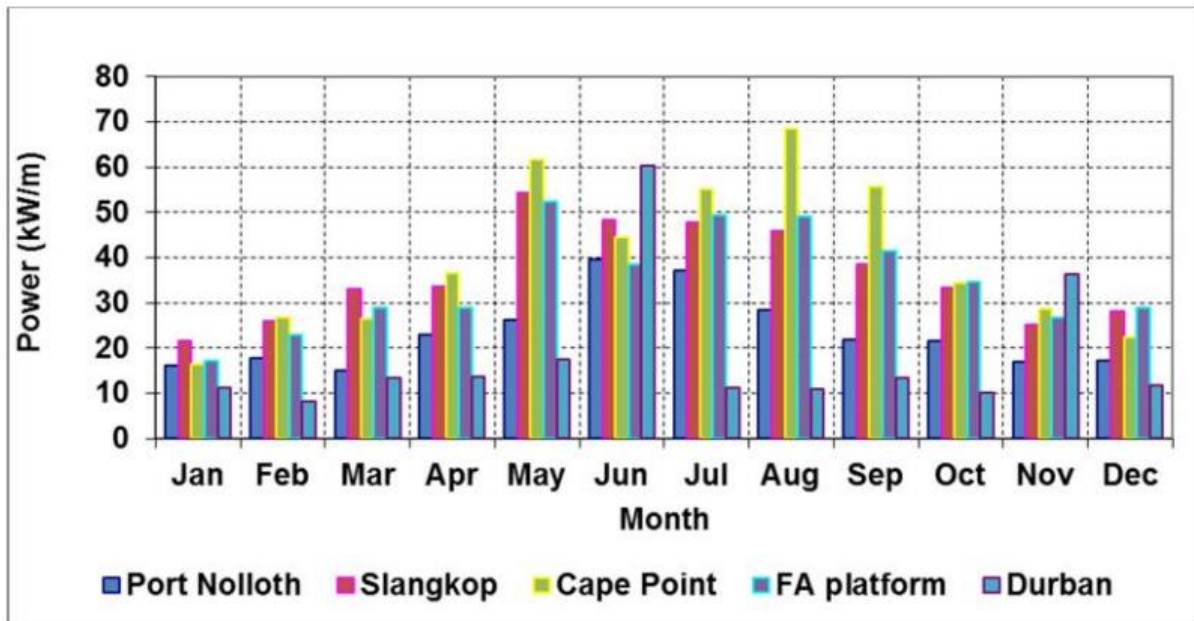


Figure 31: Wave power monthly standard variation for the different stations

## 7.2. Model hind cast and observed data comparison

Comparisons were made between the model output and the actual data recorded at Cape Point to see how close they came to being accurate. The coordinates 250 00 East (6 211 500 North) are the closest grid point in the model to the Cape Point recording station. The station's grid point is located 390 meters south of Cape Point, at a depth of 78 meters (compared to 70 meters at Cape Point). From July 2000 to July 2006, the recording period of the Cape Point recording station and the Base NCEP data overlapped, as shown in 4.3. Information gathered within this time frame will be used for analysis. The reliability of both the NCEP wave forecast and the SWAN wave model is evaluated here (Joubert, 2013b).

The monthly observed wave data recorded at Cape Point is compared with the hindcast data relocated from Base to the model grid point closest to Cape Point in the next section.

### 7.2.1. Monthly wave power distribution at Cape Point was compared with data from SWAN hind cast transmissions at the latter recording point.

Statistical features of monthly wave power at the Cape Point recording station and the closest model grid point to Cape Point are shown in Figure 32 below for the six-year overlapping recording period. Figure 33 shows that the model overestimates wave power by a lot in the winter months of June, July, and August. This is because the estimated wave power is much higher than the observed wave power at the Cape Point recording station.

Monthly average wave power is shown in Table 9 below, along with the percent discrepancy between anticipated and observed data. Table 9 shows that the model may exaggerate monthly average wave power by as much as 9% during the colder months of June and July and can underestimate it by as much as 6% during the warmer months of February. There is a 5% overestimation of annual average wave power in the model(de Vos, Vichi and Rautenbach, 2021)(Joubert, 2008).

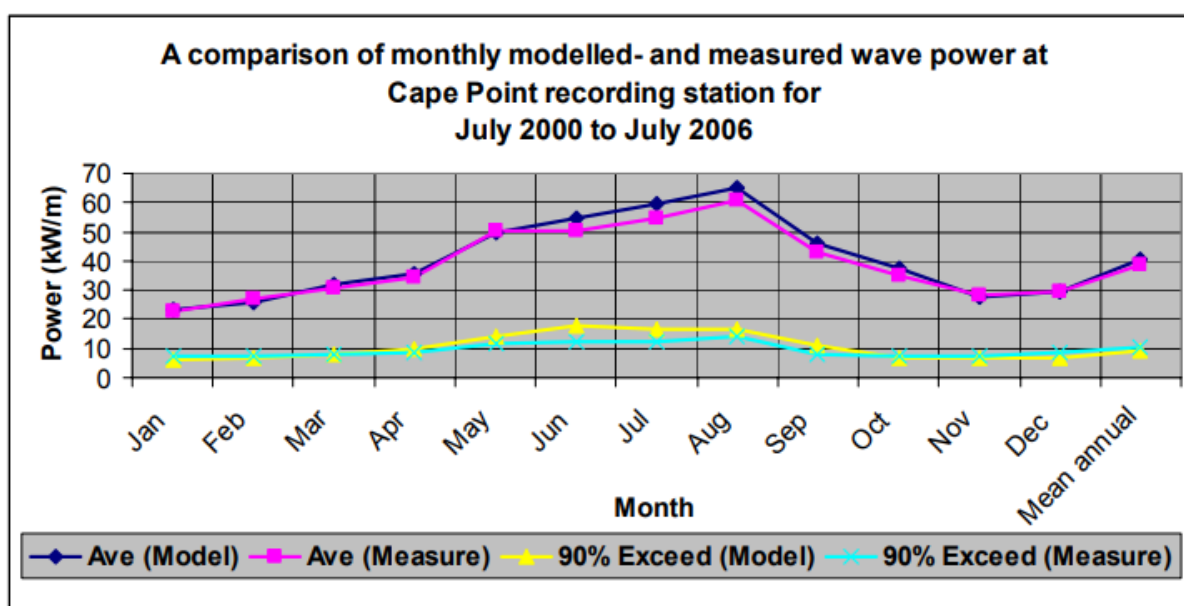


Figure 32: Wave power is measured and predicted monthly.

Table 9: Average monthly wave power of observed and simulated data that differs by a certain percentage

Jan	Feb	Mar	Apr	May	Jun	Jul	Aug	Sep	Oct	Nov	Dec	Mean annual
5%	-7%	4%	-2%	8%	8%	10%	7%	9%	6%	-3%	2%	6%

Comparing the model's output to the likelihood that the wave power of the recorded data from the Cape Point recording station will surpass that value allowed for further examination of the model's accuracy. Figure 32 below shows the likelihood that the measured and modelled wave power will surpass that value. In accordance with Figure 33, the model's estimations of wave power are accurate enough for the study's purposes, although they are slightly inflated for the majority of the data, with a chance of exceedance ranging from 20 to 80%. For the observed and modelled data, Table 9 below shows the wave strength of severe occurrences with modest likelihood of exceeding 2% and 6%.

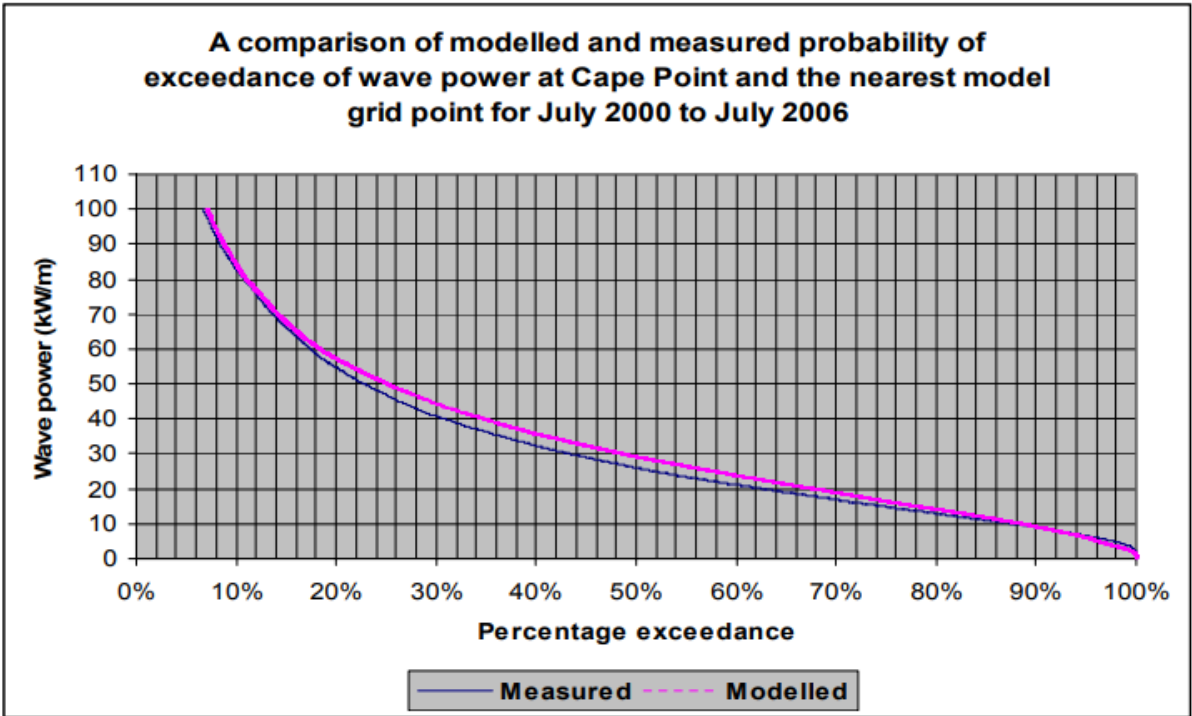


Figure 33: Wave power statistics recorded at the Cape Point recording station and the likelihood of exceeding it (hind cast data transferred)

## 8. Chapter Eight: Conclusion and Recommendations

### 8.1. Conclusion

As for the conclusion to commercialise and industrialise ocean energy development technologies, all parties, including the government, investors, engineers, and technicians, must work together to resolve economic concerns. The majority of ocean energy development technologies have yet to be commercialised. This is because of the properties of ocean energy: When compared to traditional energy sources, they are relatively unstable and have a low energy density. As a result, when compared to traditional resources, ocean energy has a price disadvantage. However, as the scale of development expands, ocean energy begins to show clear advantages.

As illustrated in Fig. 1, the generation cost of ocean energy will be even lower than that of a coal-fired plant, indicating robust price competition. Furthermore, because the operating costs of ocean energy utilisation projects are generally low, ocean energy will have a bright future if its stability is improved. Now is an excellent time to invest in ocean energy. Ocean energy will grow in the future, thanks to government backing and the efforts of all parties. It's logical to suppose that today's wind energy will be tomorrow's ocean energy.

The purpose of this section is to provide a snapshot of the available information on ocean currents and wave energy along the South African coast. This analysis will focus on the Agulhas Current since previous research has indicated that the typical flow rates of the Benguela Current are insufficient to power marine turbines. Since the Benguela Current's typical speeds range from 0.11 to 0.23 m/s and its transports from 15 to 20 Sv<sup>1</sup>, it is not strong enough to power naval turbines and will not be explored further. While the Benguela Current has transfer values of about 60 SV, the Agulhas Current is closer to 70 SV.

In particular, South Africa's major ports needed access to real-time wave and wind data in order to optimize vessel operations. At the request of the Transnet National Ports Authority, the CSIR constructed the Integrated Port Operation Support System (IPOSS) at all of the major ports shown in Figure 6. Several wave stations along the South African coast were placed in strategic locations, such as near harbors and offshore buildings, and are successfully maintained and monitored as part of the CSIR wave recording network, also known as the

CSIR Wave Net. When it comes to measured wave data, this is still the gold standard in South Africa.

Therefore, it is evident that the emergence of ocean energy generation has posed serious environmental challenges to aquatic life, including the induction of an electromagnetic field in the ocean water due to current flowing through the cables; the interference with water currents and waves from new technological structures submerged in the ocean; and the displacement and destruction of the natural habitat of benthic organisms. More research is needed to reduce the environmental impacts discovered during commissioning, decommissioning, and operation.

Case studies were carried out to assess the growth of ocean energy in South Africa and the model's application; the findings were positive, as summarized in Chapter 4. It was decided that the model could be used and was relevant, and its flaws were pointed out.

- The relevance analysis showed that the model didn't take into account a wide enough range of possible environmental and social effects.
- The laws only give basic information about things that might have big environmental or social effects. For example, they don't say how much more ambient noise can be made before it hurts ocean animals in a big way.
- It was found that the details of the electrical network sub-system were important to the conversion technology itself and could not be dealt with separately.
- Since there hasn't been enough time for a thorough techno-economic analysis, the Levelized Cost of Energy (LCoE) cannot be used to compare the viability of ocean energy in South Africa to that of other renewable and non-renewable energy sources.

## 8.2. Recommendations for further research and improvements

In light of the study's results, the following suggestions are offered for realizing this description of the South African wave power resource:

- Indicators of wave power conditions may be used to describe the South African wave power climate as a consequence of this study. The findings might be utilized to locate

WEC units in research area locations where wave power is concentrated. It was demonstrated that while the model significantly overestimates the wave power resource in shallow water, it forecasts the resource for wave power offshore appropriately. As a result, correction factors may be created for contemporaneous  $T_p$  and  $D_p$  readings and used to the study's output to more accurately estimate the wave power resource in shallow water areas. Additional numerical modelling is necessary for thorough wave farm design, particularly for survival evaluations. This type of study will also offer more precise estimations of wave strength in shallow water situations (less than approximately 50 m).

- This will be a continuous iterative process. Research should also be done in terms of regulations to establish applicable thresholds that will improve the measurement and evaluation of the above mentioned environmental and social criteria, for example, the magnitude of excessive electromagnetic frequencies being generated by the additional devices or cabling should be limited by specific regulations.
- The electrical network sub-system should be eliminated and integrated into the conversion technology subsystem of the model. The model has laid the foundation of a comprehensive and detailed framework on how to conduct techno-economic studies and it is thus recommended that the 12th INCOSE SA Systems Engineering Conference ISBN 978-0-620-72719-8 Page 114 model be adapted to also be able to conduct such detailed and comprehensive techno economic studies on other potential energy technologies. The cost model presented in the model should also be evaluated and improved where applicable. Lastly it is recommended to continue to follow and record the progress of ocean energy development by periodically applying the developed model to evaluate the technologies and compare it to other energy technologies.
- Different statistical metrics of wave power may be retrieved from the results of this study after the identification of possible wave farm sites in the study region. Any one of the 45 991 grid points can have its wave power distribution analysed in a manner akin to the measured wave power analysis of this study.



## Reference

- Agarwal, U. *et al.* (2022) *An Endless Source of Renewable Energy Ocean Energy* : Available at: <https://doi.org/10.4018/978-1-6684-4012-4.ch006>.
- Apunda, M. and Nyangoye, B. (2018) 'Environmental Challenges for Ocean Energy Generation', *International Journal of Development Research*, 08(07), p. pp.21744-21748.
- Baumgardner, S.E. (2016) 'Quantifying Galloway: Fluvial, Tidal and Wave Influence on Experimental and Field Deltas A DISSERTATION SUBMITTED TO THE FACULTY OF UNIVERSITY OF MINNESOTA BY'.
- Blake, D. (2010) 'Sea Level Rise and Flood Risk Assessment for a Select Disaster Prone Area Along the Western Cape Coast. Phase 1 Report: Eden District Municipality Sea Level Rise and Flood Risk Literature Review. Prepared by Umvoto Africa (Pty) Ltd for the Provincial Gove', *Department of Environmental Affairs and Development Planning*, (769/1/1/2010), p. 33.
- Booij, N., Ris, R.C. and Holthuijsen, L.H. (1999) 'A third-generation wave model for coastal regions 1. Model description and validation', *Journal of Geophysical Research: Oceans*, 104(C4), pp. 7649–7666. Available at: <https://doi.org/10.1029/98JC02622>.
- Chakraborty, S. *et al.* (2021) 'An overview of ocean energy policies across the world', *Water and Energy International*, 64(5), pp. 38–46.
- Chen, J. *et al.* (2022) 'A Comparative Method for Assessment of Sustainable Energy Development across Regions: An Analysis of 30 Provinces in China', *Energies*, 15(15). Available at: <https://doi.org/10.3390/en15155761>.
- Committee, T.N. and Engineering, O. (2012) *Engineering Guidelines for working with the Australian coast in an ecologically*.
- DFFE (2021) 'National Data and Information Report for Marine Spatial Planning Knowledge Baseline for Marine Spatial Planning in South Africa'.
- Elizabeth, P. (2017) 'SAMss', (July).
- Fairhurst, J. (2015) 'Modelling and Design of an Oscillating Wave Energy Converter by', (December).
- Farrok, O. *et al.* (2020) 'Electrical power generation from the oceanic wave for sustainable advancement in renewable energy technologies', *Sustainability (Switzerland)*, 12(6). Available at: <https://doi.org/10.3390/su12062178>.
- Ghosh, T.K. and Prelas, M.A. (2011) 'Energy Resources and Systems', *Energy Resources and Systems*

[Preprint], (January 2001). Available at: <https://doi.org/10.1007/978-94-007-1402-1>.

Griekspoor, W. (1981) 'Ocean thermal energy conversion', *Resources and Conservation*, 7(C), pp. 49–60. Available at: [https://doi.org/10.1016/0166-3097\(81\)90019-5](https://doi.org/10.1016/0166-3097(81)90019-5).

Hasager, C.B., Astrup, P. and Nielsen, P. (2007) 'QuikSCAT and SSM/I ocean surface winds for wind energy', *International Geoscience and Remote Sensing Symposium (IGARSS)*, pp. 3507–3512. Available at: <https://doi.org/10.1109/IGARSS.2007.4423602>.

Hassan, M. and Bora, S.N. (2019) 'Diffraction of water waves by a finite circular hollow cylinder in water of infinite depth', 21, pp. 119–135.

Hsu, Y.L. *et al.* (2008) 'Validation Test Report for Delft3D', *Naval Research Laboratory*, (February 2008), pp. 1–42.

Imamura, J., Takagi, K. and Nagaya, S. (2019) 'Engineering analysis of turbulent flow measurements near Kuchinoshima Island', *Journal of Marine Science and Technology (Japan)*, 24(2), pp. 329–337. Available at: <https://doi.org/10.1007/s00773-018-0573-z>.

Jak McCarroll, R. *et al.* (2018) 'Wave and tidal controls on embayment circulation and headland bypassing for an exposed, macrotidal site', *Journal of Marine Science and Engineering*, 6(3). Available at: <https://doi.org/10.3390/jmse6030094>.

Johnson, D. and Fourie, C.J.S. (2012) 'An overview of energy efficiency in South African hard rock mining AN OVERVIEW OF ENERGY EFFICIENCY IN SOUTH AFRICAN HARD', (July 2014). Available at: <https://doi.org/10.1109/SAEEC.2012.6408583>.

Joubert, J.R. (2008) 'An investigation of the wave energy resource on the south african coast, focusing on the spatial distribution of the south west coast', (March), p. 183.

Joubert, J.R. (2013a) 'Design and development of a novel wave energy converter', *Ph.D. thesis, Stellenbosch University, Western Cape, South Africa*, (December), p. 150.

Joubert, J.R. (2013b) 'Design and development of a novel wave energy converter', *Ph.D. thesis, Stellenbosch University, Western Cape, South Africa*, p. 150.

Lieber, L. (2021) 'Reducing Environmental Uncertainties for Sustainable Ocean Energy Dr Lilian Lieber', (January).

Magagna, D., Monfardini, R. and Uihlein, A. (2018) 'Ocean energy in europe: Assessing support instruments and cost-reduction needs', *International Marine Energy Journal*, 1(1), pp. 1–7. Available at: <https://doi.org/10.36688/imej.1.1-7>.

Maristany, L. *et al.* (2012) 'GECCO ocean energy system', in *OCEANS 2012 MTS/IEEE: Harnessing the Power of the Ocean*. Available at: <https://doi.org/10.1109/OCEANS.2012.6404787>.

Martínez, M.L., Silva, R. and Garcia, J. (2021) 'How Can We Use Ocean Energy to Generate Electricity?', *Frontiers for Young Minds*, 9. Available at: <https://doi.org/10.3389/frym.2021.609510>.

Meyer, I. *et al.* (2013) 'Assessment of the Ocean Energy Resources off the South African Coast', 27(April), pp. 1–65.

Michiorri, A. *et al.* (2015) 'Forecasting for dynamic line rating', *Renewable and Sustainable Energy Reviews*, 52, pp. 1713–1730. Available at: <https://doi.org/10.1016/j.rser.2015.07.134>.

Neil Habig, S.E. and T. deWolff (2004) 'New Jersey Offshore Wind Energy: Feasibility Study, Final Version (With NJ DEP Comments)', (December). Available at: <http://hdl.rutgers.edu/1782.1/NJEDL.Report.n3754>.

Niekerk, J. R. Joubert, J.L. van (2013) 'South African Wave Energy Resource Data', 27(May). Available at: [http://www.crses.sun.ac.za/files/research/publications/technical-reports/SANEDI\(WaveEnergyResource\)\\_edited\\_v2.pdf](http://www.crses.sun.ac.za/files/research/publications/technical-reports/SANEDI(WaveEnergyResource)_edited_v2.pdf).

Ogers, W.E.R.R. (2004) 'Validation Test Report for the Simulating Waves Nearshore Model ( SWAN ): Cycle III , Version 40 . 11', *Test [Preprint]*, (March).

Pereiras, B., Valdez, P. and Castro, F. (2014) 'Numerical analysis of a unidirectional axial turbine for twin turbine configuration', *Applied Ocean Research*, 47, pp. 1–8. Available at: <https://doi.org/10.1016/j.apor.2014.03.003>.

Richardson, D. (2019) 'Multi-Axis Point Absorber Wave Energy Converters', (May).

Ringwood, J. (2010) 'Practical challenges in harvesting wave energy', *Journal of Ocean Technology*, 5(2), pp. 73–91.

Sahed, A. and Ismail Alnaimi, F.B. (2014) 'Full-scaled impulse turbine performance prediction using numerical simulation', *Pertanika Journal of Science and Technology*, 22(1), pp. 289–306.

Schumann, E. (2014) 'Wind-driven mixed layer and coastal upwelling processes off the south coast of South Africa Wind-driven mixed layer and coastal upwelling processes off the south coast of South Africa', (November). Available at: <https://doi.org/10.1357/002224099321549639>.

Schumann, E. (2015) 'Sea level variability in South African estuaries Sea level variability in South African estuaries', (March 2013). Available at: <https://doi.org/10.1590/sajs.2013/1332>.

Schumann, E. (2017) 'Renewable ocean energy in South Africa Oceans and Coasts Resource Valuation Programme Project 2 An Assessment of the Potential of Ocean Based Renewable Energy to the South African Economy Prepared for the', (February).

SEA (2017) 'Sustainable energy solutions for South African local government: a practical guide', *Sustainable Energy Africa*, p. 24. Available at: <https://doi.org/10.1016/j.braindev.2010.03.002>.

Singh Randhawa, J. (2015) 'Ocean Energy: The Future of Renewable Energy', (August), pp. 1–12. Available at: <https://www.researchgate.net/publication/280937085>.

Solution, I., Machine, S.V. and Algorithm, C. (2019) 'Performance Evaluation of Energy Transition Based Ideal Solution and Support Vector Machine'.

'Study of an Electromagnetic Ocean Wave Energy' (no date).

Terao, Y. and Sakagami, N. (2014) 'A feasibility study on the ocean higher altitude strong wind energy utilization system', *Oceans 2014 - Taipei* [Preprint]. Available at: <https://doi.org/10.1109/OCEANS-TAIPEI.2014.6964357>.

Treasury (2018) 'Economic transformation, inclusive growth, and competitiveness: Towards an Economic Strategy for South Africa Prepared by Economic Policy, National Treasury', *World Economic Forum*, pp. 1–62.

Treffers, R. (2009) 'Wave-Driven Longshore Currents in the Surf Zone - Hydrodynamic validation of Delft3D', p. 137.

de Vos, M., Vichi, M. and Rautenbach, C. (2021) 'Simulating the coastal ocean circulation near the cape peninsula using a coupled numerical model', *Journal of Marine Science and Engineering*, 9(4). Available at: <https://doi.org/10.3390/jmse9040359>.

Weecs, T., Archipelago, M. and Girard, M. (2009) 'Hydrodynamic Modeling of Heaving Systems for Wave Energy Conversion Pedro Tomás Pestana Mendonça Abstract ':

Zou, S. (2018) 'Digital Commons @ Michigan Tech Optimal Control of Wave Energy Converters'.

